LA100 EQUITY STRATEGIES

Chapter 15. Air Quality and Public Health

FINAL REPORT: LA100 Equity Strategies

Qiao Yu,[1] Yun Lin,[2] Yueshuai He[3], Yu Gu[2], Jiaqi Ma[3], and Yifang Zhu[1]

1 Department of Environmental Health Sciences, Fielding School of Public Health, University of California, Los Angeles
2 Joint Institute for Regional Earth System Science and Engineering and Department of Atmospheric and Oceanic Sciences, University of California, Los Angeles
3 Department of Civil and Environmental Engineering, Samueli School of Engineering, University of California, Los Angeles, Los Angeles

LA DWP UCLA

Chapter 15. Air Quality and Public Health

FINAL REPORT: LA100 Equity Strategies

Authors:

Qiao Yu, Yun Lin, Yueshuai He, Yu Gu, Jiaqi Ma, and Yifang Zhu

May 2023

Produced under direction of the Los Angeles Department of Water and Power by members of the Department of Environmental Health Sciences, Fielding School of Public Health, the Joint Institute for Regional Earth System Science and Engineering and Department of Atmospheric and Oceanic Sciences, and the Department of Civil and Environmental Engineering, Samueli School of Engineering at the University of California Los Angeles.

Acknowledgements

This work was supported by Sustainable LA Grand Challenge program and the Los Angeles Department of Water and Power. The views, opinions, findings, and conclusions or recommendations expressed in this paper are strictly those of the authors. They do not necessarily reflect the views of funding agencies and/or authors' affiliated institutes.

Cover photo from iStock 960280378

1 Introduction

The transportation sector is the largest contributor to climate change and air pollution in California, accounting for approximately 50% of the state's greenhouse gas (GHG) emissions, nearly 80% of nitrogen oxide (NOx) pollution, and 90% of diesel particulate matter (PM) pollution[1,2]. Exposure to traffic-related air pollution (TRAP) has been consistently linked to increased risks of respiratory and cardiovascular diseases, preterm birth, cognitive function, and premature death, posing a significant health concern that necessitates the attention of policymakers and the public[3–5]. Clean vehicles, particularly zero-emission vehicles (ZEVs), produce no tailpipe emissions compared to conventional gasoline and diesel vehicles[6,7]. Thus, the transition towards clean vehicles presents an opportunity to improve air quality and yield health benefits[8,9].

Policymakers worldwide have committed to accelerating the transition to clean vehicles, leading to the implementation of various regional policies supporting these goals[10,11]. For instance, the European Union has outlined a plan to strive towards achieving 100% sales of ZEVs by 2035, with the goal of achieving this target no later than 2040[12]. China has set ambitious targets for clean vehicle adoption, aiming for electric and plug-in hybrid vehicles to account for 25% of all new car sales by 2025[13]. The United States has a patchwork of clean vehicle transition policies, with some states offering more incentives for clean vehicles than others[14]. California, which is the largest market for new cars in the country, has set a goal including putting 5 million ZEVs on the road by 2030 and achieving 100% ZEVs sales for new passenger cars and light trucks by 2035 through Executive Orders B-48-18 and N-79-20, respectively[15]. To promote the transition towards clean vehicles, governments often employ financial incentives, such as tax credits, rebates, and subsidies[16]. Such policy instruments are designed to alleviate the financial burden associated with purchasing clean vehicles. Moreover, the development of charging infrastructure is an essential part of the clean vehicle transition, and governments frequently provide financial incentives to support its expansion[17–19].

In Los Angeles (LA), addressing air pollution has been an ongoing challenge for many decades, with a particular focus on emissions from motor vehicles[20–22]. Disadvantaged communities (DACs) in the city are confronted with a wide range of socio-economic challenges, including high levels of poverty, unemployment, and limited access to essential healthcare services[23]. Furthermore, DAC residents are more likely to live near-roadway, which exposes them to higher levels of TRAP, ultimately resulting in environmental inequities[24–28]. Although previous studies have quantified the ambient air quality and health benefits linked to ZEVs adoption to some extent, there is a crucial knowledge gap in the literature on evaluating the distribution equity of air quality and health benefits during the transition to clean vehicles from an environmental justice perspective[29–31].

In this study, we build upon the previous LA100 study, which aimed for the transition to 100% renewable energy in LA City, and introduce a new focus on Equity Strategies. This new focus aims to ensure a just transition by investigating the potential environmental and public health benefits of replacing conventional vehicles with ZEVs in the city of LA, especially among DACs. We first utilize state-of-the-art methods to estimate future emission trends under different scenarios, with a focus on ZEVs disparity among DACs. A personal trip-level transportation model is used to generate precise spatial emission patterns for the on-road sector under different ZEVs distribution scenarios. We then simulate consequent changes in ambient particulate matter with an aerodynamic diameter less than or equal to 2.5 micrometers ($PM_{2.5}$) and ozone (O_3) concentrations using a high-resolution chemical transport model at about 1 km x 1 km. Finally, we assess the related public health benefits and monetized economic benefits in the city of LA using racial and ethnic specific concentration-response data.

This new study emphasizes the importance of not only transitioning to cleaner energy sources but also ensuring that the benefits of this transition are equitably distributed among all communities, particularly those that have been historically underserved. By evaluating the potential health and economic impacts of increased ZEVs adoption, this study provides valuable insights for policymakers, stakeholders, and communities as they work together to create a more sustainable and equitable future for the city of LA.

2 Results

To gain a deeper understanding of how the adoption of light-, medium-, and heavy-duty ZEVs by 2035 will impact various communities, particularly those that are disadvantaged, we developed three distinct future scenarios:

(1) **Disparity:** a 2035 ZEVs Disparity scenario that maps emission reductions based on varying ZEVs ownership adoption rates;
(2) **Equity:** a 2035 ZEVs Equity scenario where emission reductions in on-road transportation based on a uniform ZEVs ownership adoption rate at 50% for every census tract; and
(3) **Equity_MSS**: a 2035 ZEVs Equity scenario that emphasizes increased ZEVs usage in medium- and heavy-duty vehicles, with mobile source (both on-road and off-road) emission reductions aligned with the California Air Resources Board (CARB) 2020 Mobile Source Strategy (MSS)[1]

To assess the changes in ambient air quality for these 2035 scenarios, we use a baseline scenario reflecting the 2017 emission levels (i.e., **Base**). Table A1 in the Appendix reports the technical details for each scenario.

2.1 Emission Inventory

Figure 1 illustrates the total emission rates of all source categories for NOx and $PM_{2.5}$ in LA City in 2035, relative to the Base scenario. The figure highlights that intensive emissions, especially for NOx, are predominantly transportation-related, as they are concentrated along the transportation networks within the city. The total emissions of NOx and $PM_{2.5}$ in the Disparity scenario are reduced by 55% and 11%, respectively, relative to the Base scenario. Since the

Equity scenario is set with same total emissions as the Disparity scenario (see Table 1), both NOx and $PM_{2.5}$ emissions change only slightly (<1%) due to the offsetting changes in emissions at different locations. In the Equity_MSS scenario, the emissions are further reduced on the base of the Disparity scenario by 14% and 1% for NOx and $PM_{2.5}$, respectively. This reduction is attributed to the increased electrification of medium- and heavy-duty vehicles.

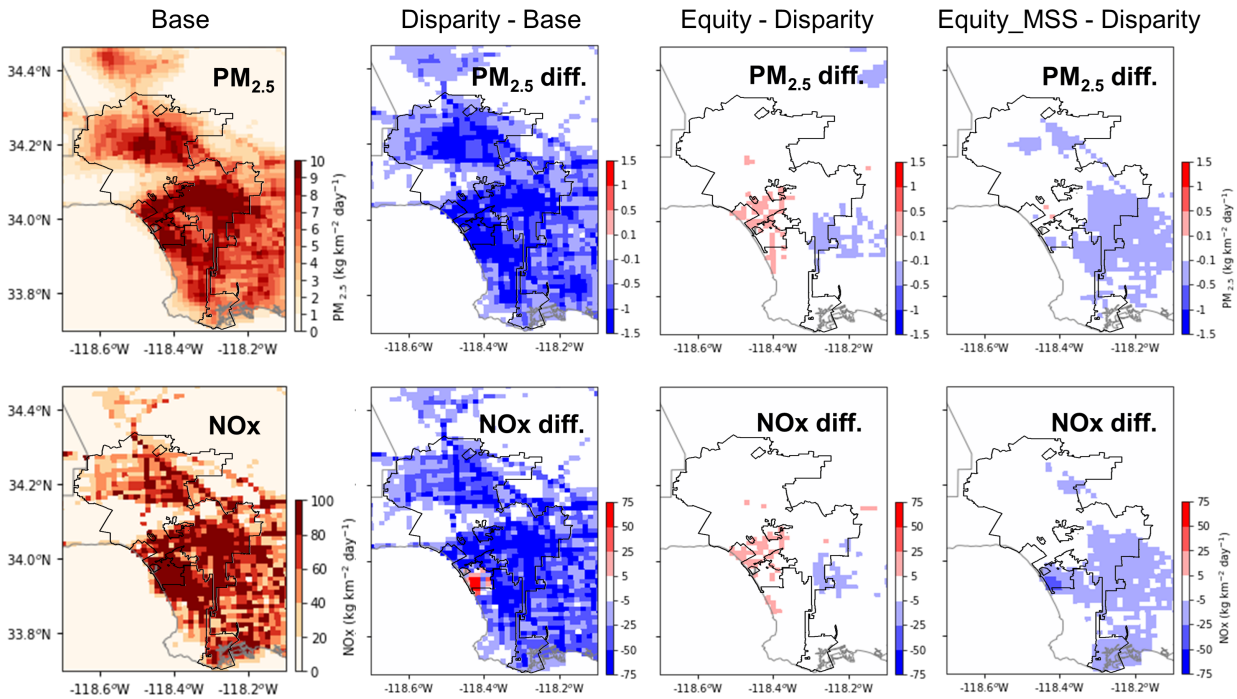

Figure 1. The total emission rates of all the source categories for $PM_{2.5}$ and NOx in LA City in 2035 relative to the 2017 Base

Black line marks LA City boundary.

Table 1 summarizes the total primary air pollutant emissions from all emissions sectors for the future. Compared to the Base scenario, the Los Angeles countywide total emissions of carbon monoxide (CO), NOx, reactive organic gas (ROG) and sulfur oxides (SOx) in the Disparity scenario are considerably reduced by 57%, 45%, 29%, and 7.7%, respectively, and the primary $PM_{2.5}$ is slightly reduced (3.1%) in 2035 relative to 2017. In 2035, ammonia (NH_3) and particulate matter with an aerodynamic diameter less than or equal to 10 micrometers (PM_{10}) emissions increased by 2.2% and 1.0%, respectively. These increases are likely associated with the economic development and population growth observed between 2017 and 2035. Compared to the Equity scenario, the Equity_MSS scenario shows slight decreases in emissions of most pollutants except for NOx. The emission of NOx in the Equity_MSS scenario is reduced by about 30% from the Equity (or Disparity) scenario. The primary $PM_{2.5}$ emission is further reduced by 3.2% in the Equity_MSS scenario.

Table 1. Pollutant-specific Emissions (tons per day) Under Base, Disparity, Equity, and Equity_MSS Scenarios and Their Relative Changes for Los Angeles County
Note that Disparity and Equity are designed with same total emission amount but different spatial distributions.

Scenarios	CO	NH_3	NOx	PM_{10}	$PM_{2.5}$	ROG	SOx
Base	1032	46	252	96	32	303	13
Disparity	446	47	138	97	31	216	12
Equity	446	47	138	97	31	216	12
Equity_MSS	425	46	97	97	30	215	12
Disparity - Base	-57%	2.2%	-45%	1.0%	-3.1%	-29%	-7.7%
Equity_MSS - Disparity	-4.7%	-2.1%	-30%	0.0%	-3.2%	-0.5%	0.0%

2.2 Changes in Ambient Air Quality

For each emission scenario, four sets of one-month-long simulations are conducted, representing the winter, spring, summer, and fall seasons for January, April, July, and October, respectively. To evaluate the overall sensitivity of ambient air quality to emission scenarios, the simulated changes in concentrations of $PM_{2.5}$ and O_3 over LA City are examined.

Figures 2 and 3 display the monthly mean spatial distributions of daily $PM_{2.5}$ and daily maximum 8-hour average (MDA8) O_3 concentrations in four representative months under various scenarios. Additionally, Figure 4 shows the citywide means of daily $PM_{2.5}$ and MDA8 O_3 concentration for each season. As shown in Figure 2, the $PM_{2.5}$ concentration hotspots (i.e., regions with high $PM_{2.5}$ concentration) over LA City are located over the city center areas and its southern part in both January and October, over the city center areas in April, and over the city center areas and its northern part in July. The LA citywide mean $PM_{2.5}$ concentrations exhibit similar seasonal variations across different scenarios, with summer being the least polluted season and winter and fall being the most polluted seasons (Figure 4A). The seasonal dependence of $PM_{2.5}$ concentration and spatial pattern reflects the seasonal variations in pollutant emissions and meteorological conditions in LA City. The sensitivity of $PM_{2.5}$ to emission scenarios exhibits little seasonal variation, with Base having the highest concentration and Equity_MSS having the lowest concentration across all seasons. The spatial patterns of O_3 are consistent across different seasons (Figure 3), with two regions of low O_3 concentration in the domain: the central areas of LA City and the coastal region next to the San Pedro Bay. The domain mean O_3 concentration over the LA City region varies by season, with the lowest concentration in winter and the highest concentration in spring (Figure 4B).

It's worth noting that over a larger simulation domain, e.g., Southern California as shown in Figure A1 in the Appendix, both simulations and observations show that the month of July has the highest inland O_3 concentration, followed by April and October, while January shows the least O_3 pollution. The seasonal distribution of simulated O_3 over Southern California differs from that in LA City, which is also evident in the observed seasonality based on the Air Quality System (AQS) measurements from the U.S. Environmental Protection Agency (EPA) (Figure A2). The seasonality shift could be attributed to the following processes: Although the summer season is generally conducive to O_3 production, the prevailing westerly and southerly winds

(Figure A3) from the ocean can dilute and blow O_3 pollution away from the coastal areas of the LA Basin towards its inland regions. The mountain ranges to the north and east could block the air flow, leading to a rapid accumulation of O_3 pollution in the mountain hill areas. Consequently, the western part of the LA Basin, where LA City is located, is cleaner than the eastern part of the Basin in July. In April and October, when there are no prevailing winds, pollution disperses more evenly in the LA Basin than in July, resulting in more O_3 pollution in LA City during these months. As for LA County and Southern California, they cover almost the entire LA Basin, including those mountain hill regions where severe pollution accumulates. Since summer produces more O_3 than other seasons, the domain-averaged O_3 concentration over LA County and Southern California is higher in July than in April and October. In summary, the spatial heterogeneity of O_3 concentration over LA Basin caused by the prevailing winds in July leads to the distinctive seasonal patterns among LA City, LA County and/or Southern California. The sensitivity of O_3 concentration to emission scenarios is similar across different seasons, with Base having the highest O_3 concentrations and Equity_MSS having the lowest concentrations.

Table 2 summarizes the citywide average of annual mean daily $PM_{2.5}$ concentrations and MDA8 O_3 in all scenarios. The annual mean values are obtained by averaging the four simulated months, as these months provide a representative view of the significant seasonal variations in emissions and meteorological conditions. The annual mean $PM_{2.5}$ concentrations over LA City are 11.5, 10.6, 10.6, and 10.2 □g m^{-3} for the Base, Disparity, Equity and Equity_MSS scenarios, respectively. Reductions in emissions of precursors to secondary $PM_{2.5}$ (e.g., NOx and VOC) result in a decrease of 0.8 □g m^{-3} (7.4%) in annual mean $PM_{2.5}$ in the Disparity relative to the Base scenario. The Equity scenario does not show any significant change in annual mean $PM_{2.5}$ concentrations, maintaining the 10.6 □g m^{-3} level that was achieved in the Disparity scenario. The Equity_MSS scenario shows a further reduction, bringing the annual mean $PM_{2.5}$ down to 10.2 □g m^{-3}. This signifies a reduction of 1.3 □g m^{-3} (11%) compared to the Base scenario.

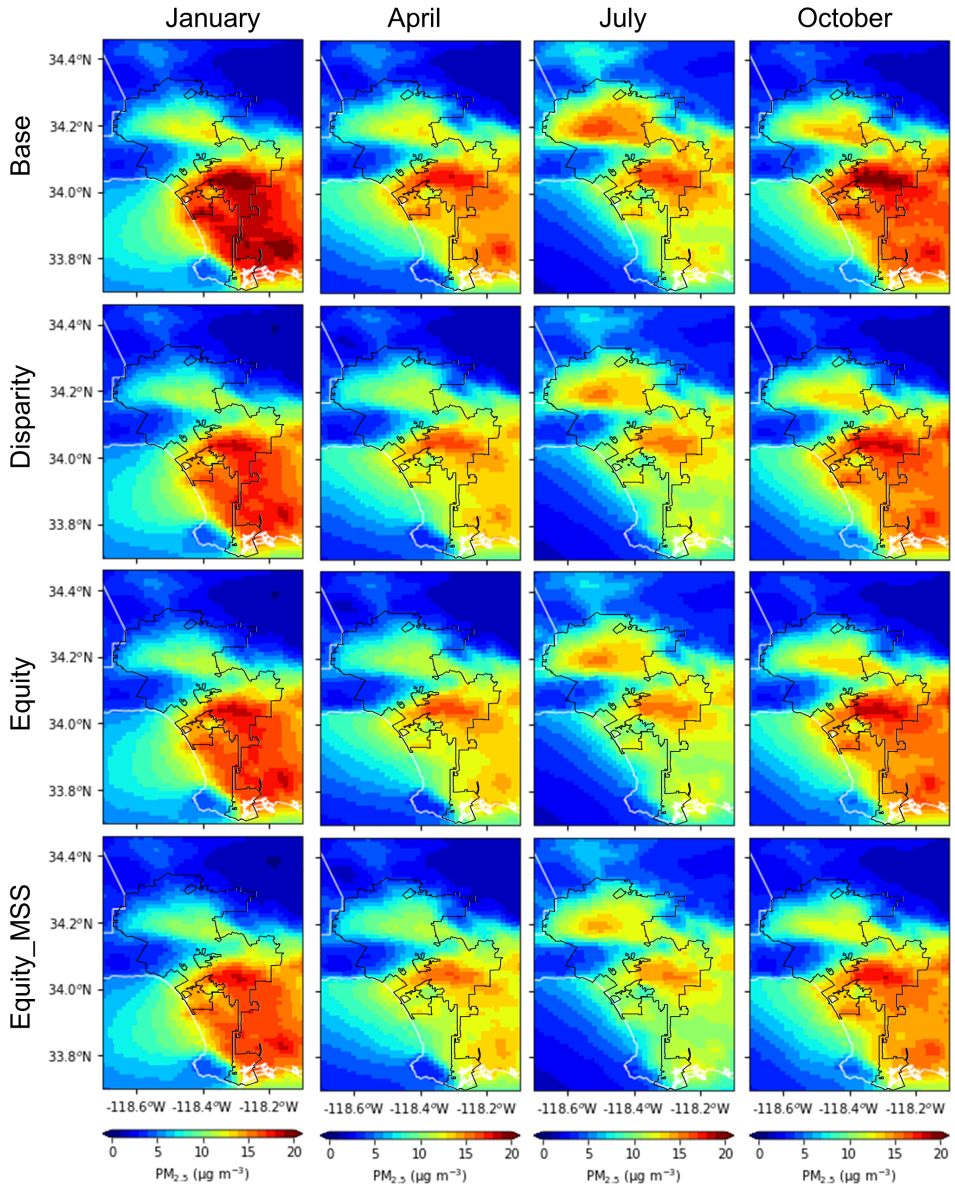

Figure 2. Monthly mean daily $PM_{2.5}$ concentrations for four representative months in LA City for Base, Disparity, Equity, and Equity_MSS

Black line marks the LA City boundary.

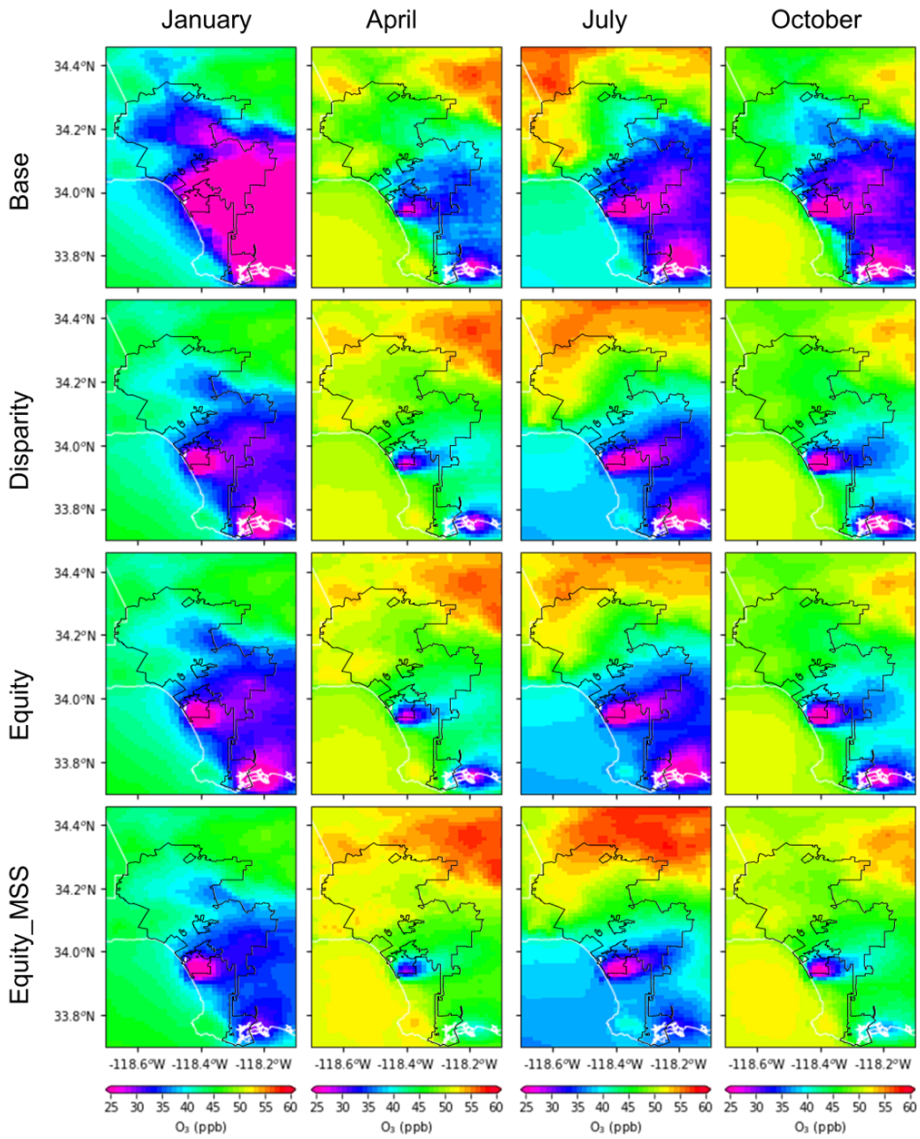

Figure 3. Monthly mean daily maximum 8-hour average O_3 concentration for four representative months in LA City for Base, Disparity, Equity, and Equity_MSS

Black line marks the LA City boundary.

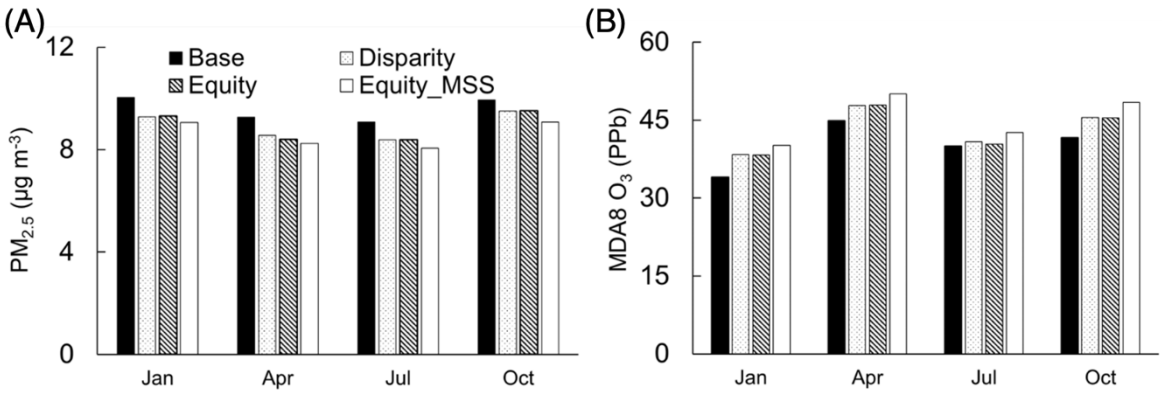

Figure 4. Monthly mean of LA City region daily $PM_{2.5}$ concentrations (A) and daily maximum 8-hour average O_3 concentrations (B) for Base, Disparity, Equity, and Equity_MSS scenarios

Table 2. Simulated LA Citywide Annual Average of Daily Maximum 8-hour O_3 and Daily $PM_{2.5}$ Concentrations for all Evaluated Scenarios

Percentages in parentheses show relative changes between different scenarios and the Base.

Pollutants	Base	Disparity	Equity	Equity_MSS
O_3 (ppb)	38	42 (+12%)	42 (+12%)	45 (+18%)
$PM_{2.5}$ (μg m^{-3})	11.5	10.6 (-7.4%)	10.6 (-7.4%)	10.2 (-11%)

In contrast, the annual mean MDA8 O_3 concentrations show an increase from the Base scenarios (i.e., in 2017) to future scenarios (i.e., in 2035), and the concentrations for the Base, Disparity, Equity, and Equity_MSS scenarios are 38, 42, 42, and 45 ppb, respectively. The O_3 concentration increases on average by 12% from Base to Disparity. The Equity scenario also has O_3 concentration of 42 ppb, maintaining the same level as the Disparity scenario. This represents the same increase of 12% in comparison to the Base scenario. The Equity_MSS scenario shows an increase to 45 ppb, which equates to an 18% rise in O_3 concentration relative to the Base scenario. The overall increase in O_3 concentrations occurs despite the reductions in NOx emissions noted above, which is because O_3 production depends on the particular ratio of the two precursors: NOx and volatile organic compounds (VOCs), and the nonlinearities of O_3 formation chemistry. Currently, LA City is generally in a transition regime whereby VOC reductions can lead to reductions in O_3, yet NOx reductions can lead to increases in O_3. It is important to note that the CARB 2020 MSS does not include a specific regulatory target for VOC reduction, which is why we did not model the VOC emission inventory change in our analysis. However, it is reasonable to assume that future VOC emissions would likely decrease in a real-world scenario, as the reduction in PM and NOx emissions is expected to be achieved through the electrification of both on-road and off-road vehicles and devices. Consequently, the increase in O_3 levels found in our simulation results might be an overestimation, as it does not account for the potential reduction in VOC emissions that would accompany the transition to electric vehicles and equipment.

Figures 5 and 6 illustrate the spatial distributions of annual mean $PM_{2.5}$ and MDA8 O_3 concentrations over LA City in the Base scenario and their changes in future scenarios. As shown in Figure 5, areas with high $PM_{2.5}$ concentrations are located in the city center while the suburban and/or rural areas in the western and northern parts of the city typically have lower levels of $PM_{2.5}$. These high $PM_{2.5}$ regions coincide with areas of larger emissions of primary

$PM_{2.5}$ and precursors to secondary $PM_{2.5}$ as shown in Figure 1. From the Base to Disparity scenarios, the $PM_{2.5}$ concentration decreases greatly over the entire LA City (Figure 5B). However, the adoption of the equal distribution of transportation emission reduction due to ZEVs implementation (i.e., the Equity scenario) results in relatively small changes in $PM_{2.5}$ concentrations (Figure 5C), with slight increase over the city center and slight decrease over the southern part of the city, corresponding to the relatively small emission changes between the two scenarios observed over the two regions (Figure 1). In the Equity_MSS scenario, additional reduction in PM precursors contributes to a further decrease in $PM_{2.5}$ concentrations from the Disparity scenario (Figure 5D).

Figure 6 shows that the O_3 concentration over the city center areas and its southern part is remarkably lower than that over its northern and western suburban and/or rural areas. This is mainly due to O_3 scavenging by nitric oxide (NO) which is emitted from traffic mainly over the urban source areas. In the Disparity scenario, O_3 levels are considerably elevated over almost all the areas in the city relative to the Base scenario, particularly over the urban centers of LA City (Figure 6B). This is consistent with the larger reduction in NOx over the urban center areas, given that LA City is still in the VOC-limited regime and the reduction in NOx results in more O_3 production. With the equal distribution of transportation emission reduction in the Equity scenario, the O_3 concentration shows slight decrease over the city center areas, consistent with the overall small positive changes in NOx emissions over there from Disparity to Equity scenarios (Figure 6C). Further reductions in certain precursor emissions (e.g., NOx in Table 1) in the Equity_MSS scenario yields even more O_3 production over the entire city (Figure 6D). Note that VOC is slightly reduced from the Disparity to Equity_MSS scenarios (see ROG emissions in Table 1), suggesting that the O_3 production over LA City is VOC-limited in the simulated future scenarios.

The DAC designation in LA City is obtained from the Senate Bill (SB) 535 DAC Designation[32]. Figures 5 and 6 also highlight the annual mean spatial distribution of $PM_{2.5}$ and MDA8 O_3 concentrations over DACs in the city. In the Base scenario, higher $PM_{2.5}$ concentrations are more frequently found over DACs than non-DACs (Figure 5), while O_3 concentrations are generally lower over DACs than non-DACs (Figure 6). The differences in $PM_{2.5}$ and O_3 concentrations between DACs and non-DACs in the Base scenario are generally consistent with the emissions contrast between the urban center areas and suburban regions in LA City.

Figure 7 shows the LA citywide mean of daily $PM_{2.5}$ and MDA8 O_3 concentrations over DACs and non-DACs under different emission scenarios. The $PM_{2.5}$ concentrations over DACs are considerably higher than those over non-DACs, on average by 3.7-4.0 □g m^{-3} (~40%), depending on the scenario examined, while the O_3 concentrations are lower over DACs than over non-DACs, on average by 4.6-6.0 ppb (~13%).

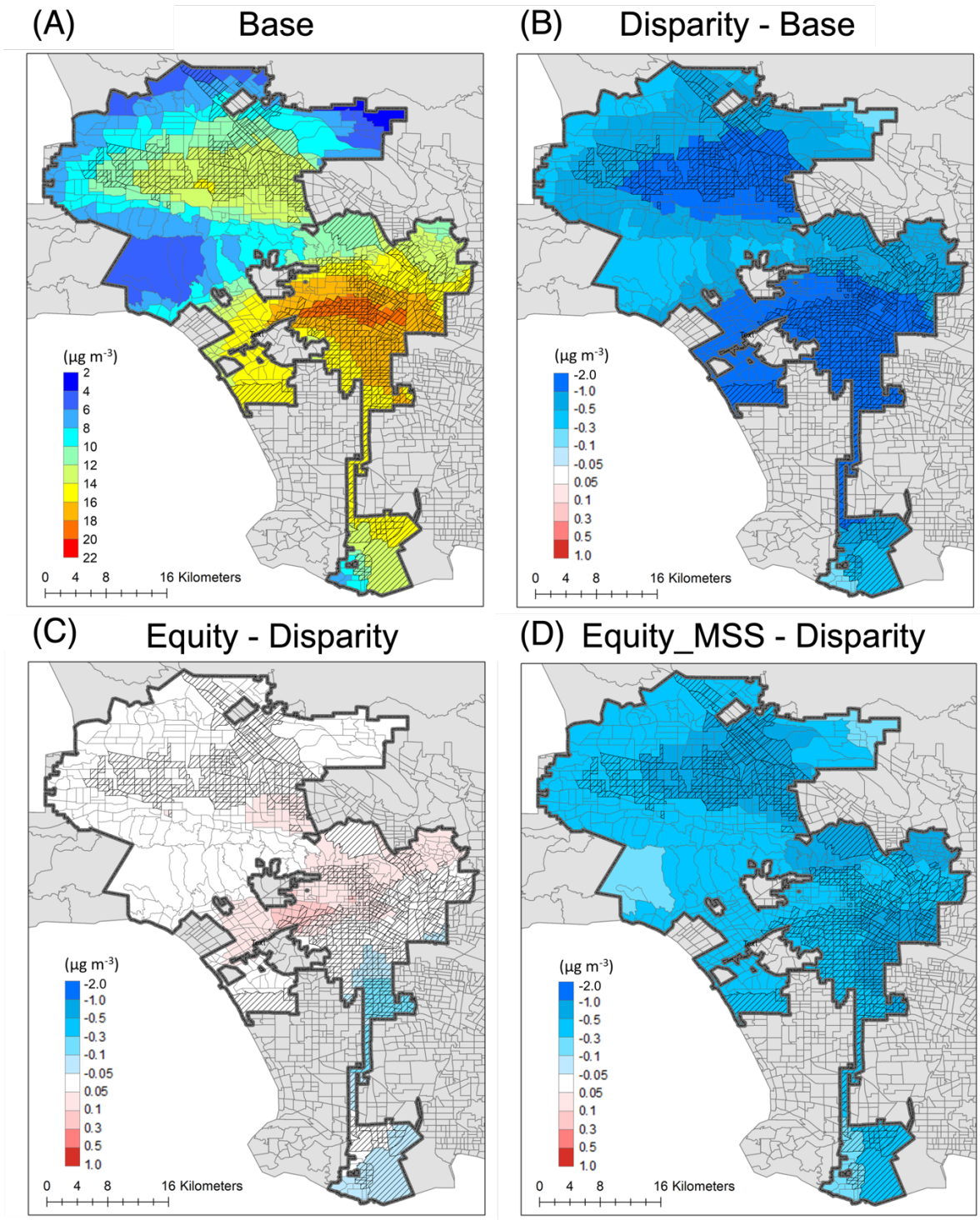

Figure 5. Annual mean daily $PM_{2.5}$ concentrations in LA City for the Base scenario (A) and the differences between Disparity and Base (B), between Equity and Disparity (C), as well as between Equity_MSS and Disparity (D)

Thick grey line marks the LA City boundary and hatch-filled areas denote disadvantaged communities in LA City.

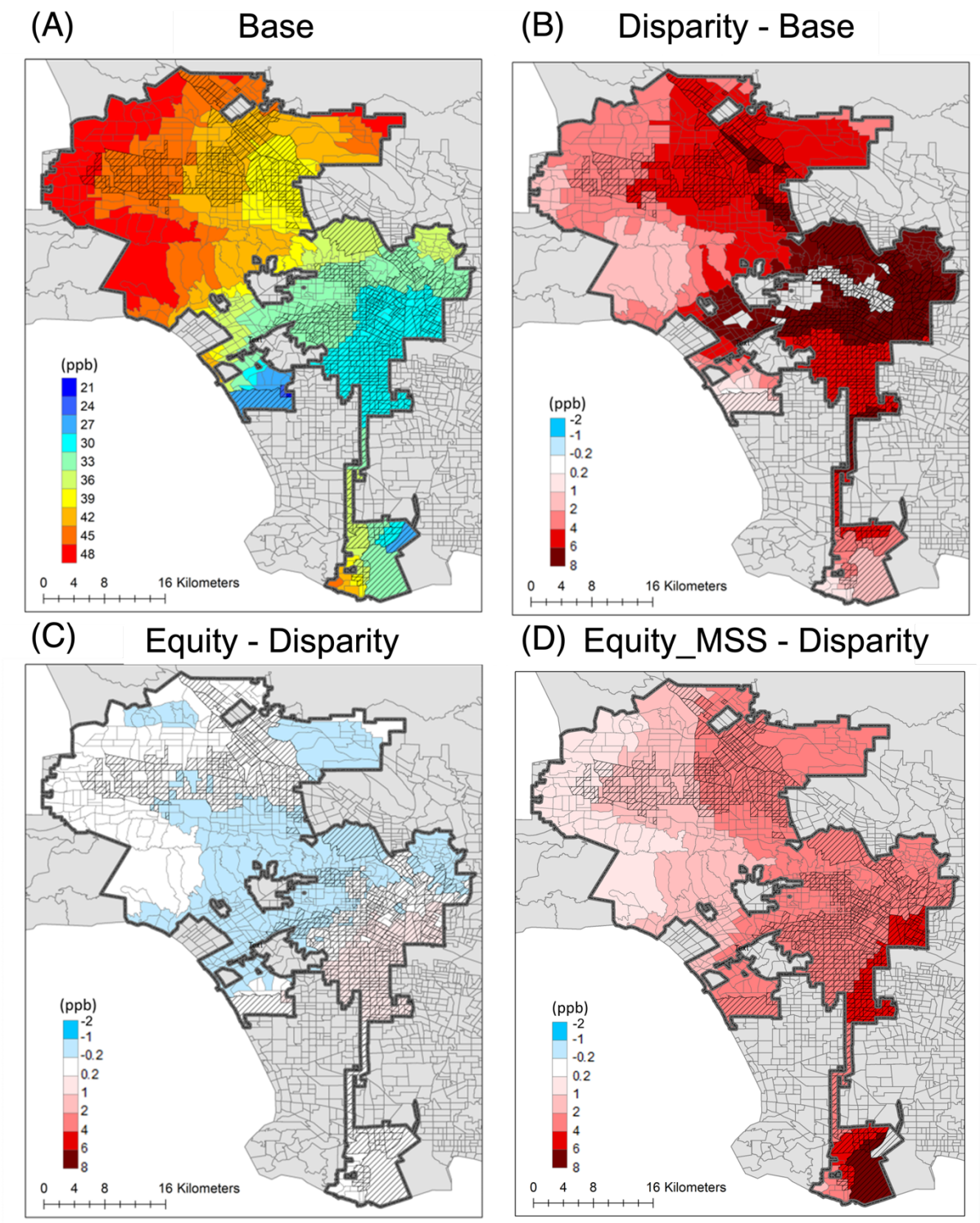

Figure 6. Annual mean daily maximum 8-hour average O_3 concentration in LA City for the Base scenario (A) and the differences between Disparity and Base (B), between Equity and Disparity (C), as well as between Equity_MSS and Disparity (D)

Thick grey line marks the LA City boundary and hatch-filled areas denote the disadvantaged communities in LA City.

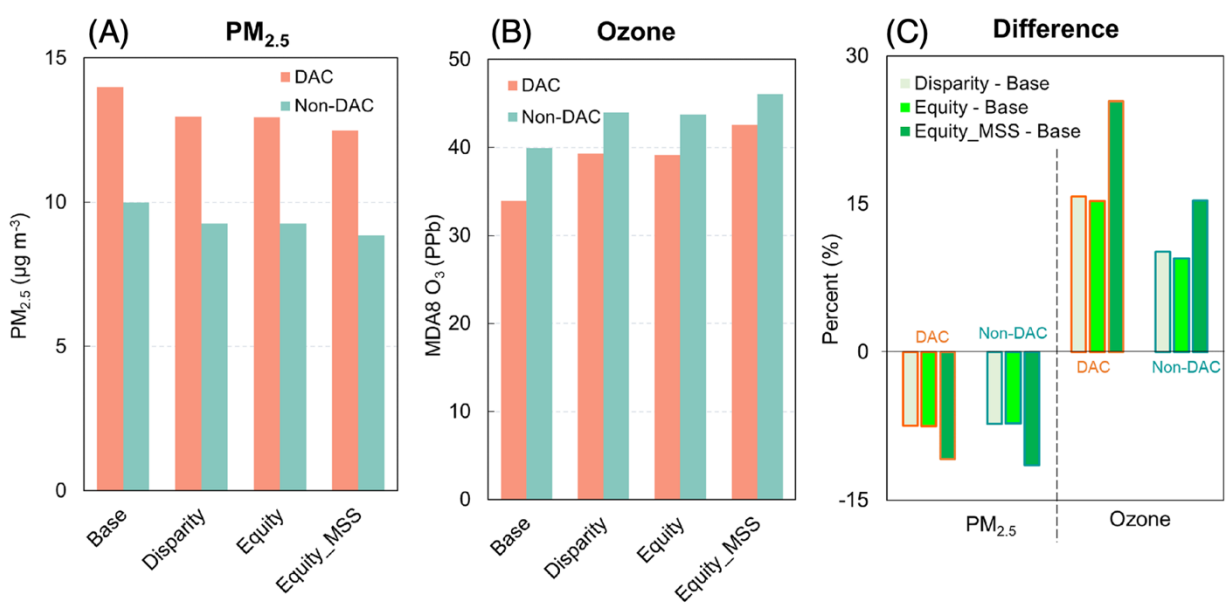

Figure 7. Community means of $PM_{2.5}$ (A) and O_3 (B) concentrations averaged over DAC and non-DACs in LA City for Base, Disparity, Equity and Equity_MSS scenarios, as well as the relative differences between the Disparity, Equity, and Equity_MSS scenarios compared to the Base scenario (C)

2.3 Public Health

Figure 8 depicts the total avoided mortality in LA City, accounting for both $PM_{2.5}$ and O_3 mortality changes. As observed in Figures 5 and 6, numerous census tracts experience health benefits due to the decrease in air pollution concentrations from 2017 to 2035. The public health benefits are more pronounced under the Equity_MSS scenario, which demonstrates the potential advantages of electrifying more medium- and heavy-duty vehicles. It is important to note that some areas exhibit disbenefits, primarily driven by the increase in O_3 concentrations in the future scenarios. Spatial distribution maps for both $PM_{2.5}$ and O_3 related mortality changes between Equity_MSS and Base scenarios are presented separately in Figure A4. This highlights the need to consider both $PM_{2.5}$ and O_3 levels when evaluating the overall impact of ZEVs adoption strategies on public health.

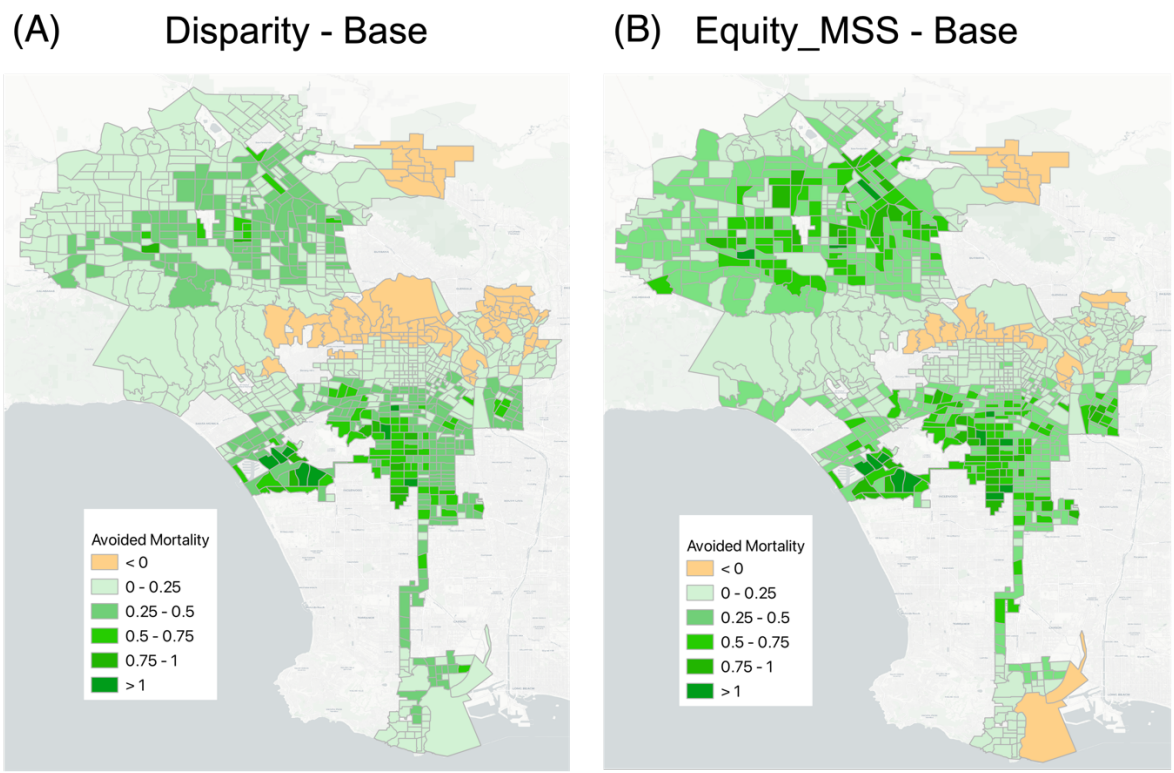

Figure 8. Total avoided mortality in LA City for the differences between Disparity and Base (A), and between Equity_MSS and Base (B)

Table 3 presents a detailed summary of the changes in both morbidity and mortality due to changes in $PM_{2.5}$ concentrations, in addition to the mortality changes highlighted in Figure 8. The changes are categorized by census tracts into DACs and non-DACs. As shown in Table 3, a total of 480 and 703 avoided mortalities attributed to $PM_{2.5}$ reduction using the uniform beta coefficient, were observed between the Disparity and Base scenarios, and between the Equity_MSS and Base scenarios, respectively. However, when the beta coefficient is adjusted based on race and ethnicity, the number of avoided mortalities related to $PM_{2.5}$ reduction increases to 567 and 831 between the same scenarios.

Figure 9 provides a more detailed analysis of the results, highlighting the underestimation of health benefits, particularly for the Hispanic population, when using a uniform exposure-response beta coefficient. When a racial and ethnic-specific beta coefficient was employed, the estimated avoided mortality increased from 169 to 270 (a 60% increase) between the Disparity and Base scenarios, and from 250 to 400 (a 60% increase) between the Equity_MSS and Base scenarios. This is due to social health disparities, such as varying access to medical services, knowledge, and coping mechanisms among different racial and ethnic groups, resulting in distinct response rates to changes in air quality. Given the high proportion of people of color in LA City, using a uniform exposure-response beta coefficient would underestimate the health benefits for this population. These findings underscore the importance of considering racial and ethnic-specific factors in health impact assessments to more accurately capture the disparities in health outcomes and ensure a more equitable evaluation of air quality improvement strategies.

Regarding morbidity, while positive health benefits are observed for $PM_{2.5}$-related respiratory emergency room (ER) visits, the overall morbidity exhibits a disbenefit due to the increase in O_3 levels. This highlights the need for a comprehensive approach to air quality management that considers the complex interplay between different air pollutants, ensuring that strategies aimed at reducing one pollutant do not inadvertently exacerbate the health impacts of another.

Table 3. Summary of Annual Health Changes Between Scenarios (Mortality and Morbidity)
Total mortality is the sum of O_3 mortality and $PM_{2.5}$ mortality.

Health Endpoints	Disparity - Base			Equity_MSS - Base		
Mortality	**Total**	**non-DAC**	**DAC**	**Total**	**non-DAC**	**DAC**
$PM_{2.5}$ Mortality (Uniform Beta)	480	214	266	703	321	383
$PM_{2.5}$ Mortality (Racial/Ethnic Specific Beta)	567	231	336	831	347	484
O_3 Mortality	-337	-155	-182	-499	-222	-277
Total Mortality	230	76	154	332	125	207
Morbidity						
$PM_{2.5}$ ER Visits, Respiratory	239	88	151	349	132	217
O_3 ER Visits, Respiratory	-677	-264	-413	-1017	-379	-638
Total Morbidity	-438	-176	-262	-668	-247	-421

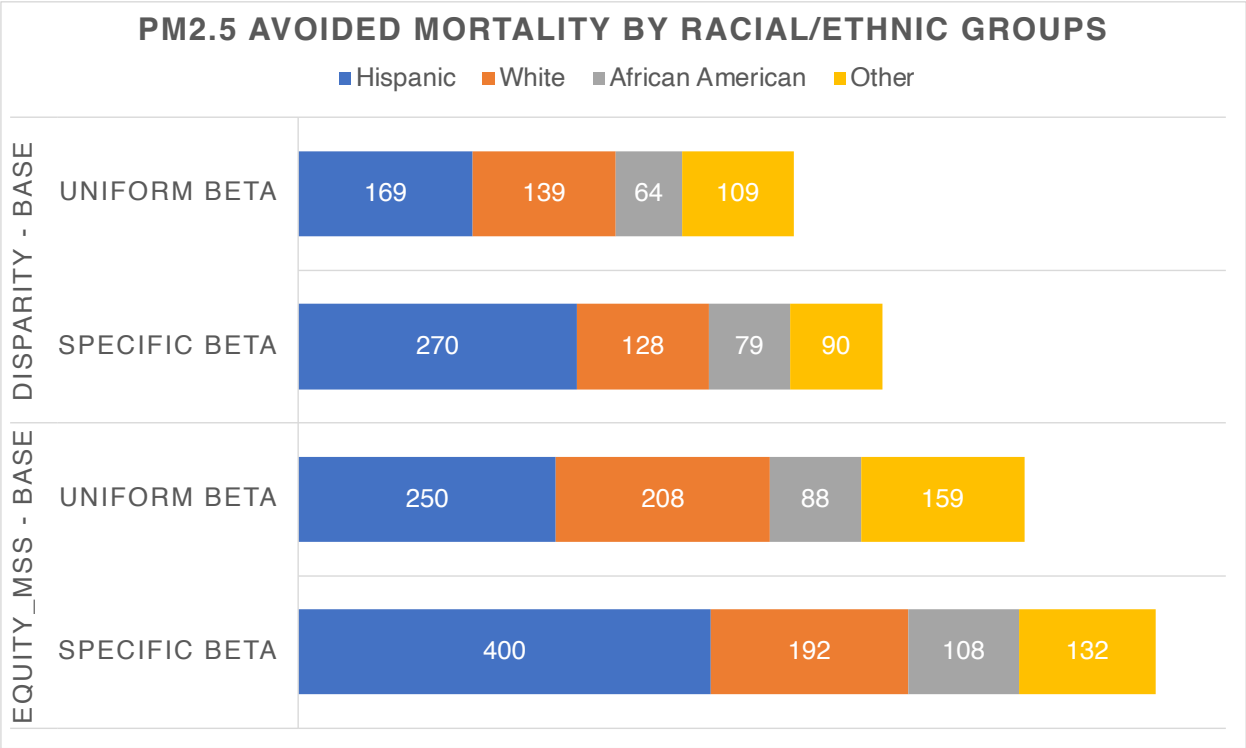

Figure 9. Differences in $PM_{2.5}$-related avoided mortality, comparing the use of uniform beta coefficients with racial/ethnic-specific beta coefficients
Upper panel represents the differences between Disparity and Base. Lower panel represents the differences between Equity_MSS and Base. This illustration highlights the disparities in health outcomes

when accounting for race and ethnicity in the analysis. Other: Asian American, Pacific Islander and Native American.

2.4 Monetized Benefits

Table 4. Monetized Health Benefits Between Scenarios for Both Mortality and Morbidity

	Disparity – Base (in 2015 million U.S. dollars)			Equity_MSS – Base (in 2015 million U.S. dollars)		
	Mean	**Low**	**High**	**Mean**	**Low**	**High**
non-DAC	$660	$90	$1,200	$1,090	$190	$1,940
DAC	$1,340	$190	$2,430	$1,800	$220	$3,310
Total	$2,000	$280	$3,630	$2,890	$411	$5,250

Table 4 summarizes the health benefits, including their 95% confidence intervals for both lower and higher estimates, associated with $PM_{2.5}$ and O_3 concentrations in LA City. The Disparity scenario, compared to the Base scenario, could result in $2 billion in health benefits, with $1.3 billion directed towards DACs. By implementing the Equity_MSS scenario, which promotes electrification of medium- and heavy-duty truck fleets and off-road equipment, $2.9 billion can be gained, with $1.8 billion benefiting DACs as compared to the Base scenario. Although the uncertainties in the valuation and health impact functions lead to a wide range of estimates, significant benefits are observed. The findings highlight the potential for targeted air quality improvement strategies to result in substantial improvements in public health and economic gains, even when considering the uncertainties in the underlying models and assumptions.

3 Discussion

In this study, we investigated the potential health impacts of various scenarios for ZEVs adoption in the city of LA. To do so, we developed three different scenarios: (1) a 2035 ZEVs Disparity scenario, (2) a 2035 ZEVs Equity scenario, and (3) a 2035 ZEVs Equity scenario with more ZEVs in medium- and heavy-duty vehicles following the 2020 Mobile Source Strategy (Equity_MSS). Our analysis focused on how these scenarios would affect DACs and other populations, taking into account the complex interplay between air pollutants such as $PM_{2.5}$ and O_3.

Our findings suggest that implementing ZEVs policies can substantially reduce $PM_{2.5}$ concentrations, leading to improved health outcomes for both DACs and non-DACs. Specifically, from the Base to Disparity scenarios, the citywide mean $PM_{2.5}$ concentration decreases by 7.4% and 7.3% over both DACs and non-DACs, respectively. There is little change between Disparity and Equity scenarios over both types of communities. However, the enhancement in ZEVs portion of medium- and heavy-duty vehicles, i.e., from the Equity to Equity_MSS scenarios, leads to 3.6% and 4.6% more reductions in $PM_{2.5}$ concentrations over DACs and non-DACs, respectively. In contrast, from the Base to Disparity scenarios, the increases in O_3 concentrations are about 16% and 10% over DACs and non-DACs, respectively. From the Disparity to Equity scenarios, the O_3 concentrations over DACs and non-DACs both show a decrease, but the decrease is relatively small, less than 1%. The O_3 concentrations

increase further from the Equity to Equity_MSS scenarios by 8.8% and 5.4% over DACs and non-DACs, respectively. In general, the implementation of ZEVs policy in the future will improve air quality in terms of the $PM_{2.5}$ over both DACs and non-DACs, and the benefits are comparable between DACs and non-DACs.

While implementing ZEVs policy can improve air quality by reducing $PM_{2.5}$, our findings suggest that it may also lead to temporary increases in O_3 pollution, particularly over DACs. This phenomenon, referred to as temporary "growing pains" in the original LA100 report, occurs when O_3 concentration increases despite NOx reduction. However, once NOx emissions reach a certain level, further reductions can result in marked improvements in O_3 levels. To address this issue, decision-makers should prioritize reducing NOx emissions further, while also working to reduce VOC emissions in conjunction with PM and NOx emissions reductions.

Our study highlights several key points.

1. Vehicle electrification offers substantial reductions in $PM_{2.5}$ that can lead to improved health outcomes for both disadvantaged and non-disadvantaged communities. This demonstrates the potential for significant improvements in public health and economic gains through targeted air quality improvement strategies.
2. Electrifying medium- and heavy-duty trucks will bring additional health benefits, particularly for DACs. Implementing the Equity_MSS scenario, which encourages the adoption of ZEVs in medium- and heavy-duty truck fleets and off-road equipment, would result in the highest health benefits in the city, with a substantial proportion of these benefits directed towards DACs.
3. The use of ethnic and racial-specific exposure-response functions can help reveal greater health benefits, particularly for the Hispanic population, than previously estimated. This underscores the importance of incorporating racial and ethnic-specific factors into health impact assessments to ensure a more equitable understanding of air quality improvement strategies.
4. To reduce O_3, it is crucial to further reduce NOx and reduce VOCs in parallel with PM and NOx emissions reduction. Since our study does not account for the potential reduction in VOC emissions that would likely accompany the transition to electric off-road equipment, the increase in O_3 levels found in our simulation results might be an overestimation. By addressing VOC emissions alongside PM and NOx, decision-makers can work towards a more comprehensive approach to air quality management.

In conclusion, our study highlights the necessity for holistic approaches to air quality control that account for the intricate interplay of various pollutants and prioritize equitable treatment for vulnerable communities. By understanding these complexities and targeting appropriate strategies, decision-makers can work towards improving public health and promoting greater equity in vehicle electrification.

4 Methods

4.1 ZEVs Adoption Trends Estimation

In this study, we applied a logistic growth model to estimate the number of light-duty ZEVs in each census tract within LA County for the year 2035. The logistic growth model is a mathematical framework commonly used to predict the adoption rate of new technologies. It describes a sigmoidal, or S-shaped, curve, representing a slow initial adoption, followed by rapid growth as the technology becomes more prevalent, and eventually leveling off as the market becomes saturated. This model has been widely applied in various fields, including technology diffusion, population growth, and resource consumption, to forecast future trends and inform decision-making processes. We utilized ZEVs ownership data for each census tract from 2015 to 2020 to establish a growth trend from EMFAC2021 v1.0.2[33], an official emission and fleet inventory database developed by the CARB. After estimating the number of ZEVs for each census tract in 2035, we adjust the total ZEVs count in LA County to achieve a final ZEVs penetration rate of 50%, in accordance with the value used in the CARB MSS report[1]. We then proportionally scale the ZEVs count for each census tract to reflect this target penetration rate.

To represent this methodology mathematically, we use the following logistic growth equation:

$$N(t) = \frac{K}{1+\frac{K-\mathrm{N0}}{\mathrm{N0}}e^{-rt}} \qquad \text{(Eq 4.1 -1)}$$

where:
N(t) is the number of ZEVs at time t (in our case, t = 2035),
K is the carrying capacity, representing the total vehicle population in 2050 (as per EMFAC data),
N0 is the initial number of ZEVs (at t = 2015),
r is the growth rate, estimated from the ZEVs ownership data from 2015 to 2020,
t is the time (in years) since the initial year.

The ZEVs fleet penetration rates at the census tract level in 2035 were subsequently utilized in both the transportation and air quality models to provide a comprehensive analysis of the air quality and health impacts of ZEVs adoption.

4.2 Transportation System Modeling

We developed an integrated transportation system model to predict the traffic volume distribution in a typical weekday for the Greater Los Angeles Area in 2035. The integrated model consists of two components: an activity-based model (ABM) to predict travel demand and an agent-based model to simulate transportation supply (infrastructure and mobility services). Each component is explicitly explained below.

4.2.1 Travel Demand Forecast

In this project, we adopted the ABM developed by Southern California Association of Governments (SCAG), which is one of the largest ABMs being implemented in the United States. The system design of SCAG ABM is presented in Figure A5 in the Appendix. At the first layer, a synthetic population is generated to represent the population in Southern California with

specific demographic and socio-economic attributes. The base year of the SCAG ABM is 2016, which indicates that the aggregated distributions of demographic and socio-economic attributes of the synthetic population are calibrated to 2016. We adopt the 2035 synthetic population from SCAG for this project. From the second to sixth layer, people's travel-related choices are predicted and coordinated based on their socio-economic attributes and the travel demand at the individual level is generated as the output. In this project, we select the travel demand of residents in Los Angeles County.

The demand of heavy-duty truck in Southern California is also modeled in the SCAG ABM. Three classes of trucks are modeled separately: light-heavy (8,500 to 14,000 lbs. gross vehicle weight (GVW); medium- heavy (14,001 to 33,000 lbs. GVW); and heavy-heavy (>33,000 lbs. GVW). The truck trips are generated according to the land use and socioeconomic data of origin and destination zones.

4.2.2 Agent-based Traffic Simulation

The transportation supply of LA County is modeled by an agent-based simulation. The model is developed based on an open-source toolkit: Multi-Agent Transport Simulation (MATSim). The movement of travelers and vehicles in a multimodal network is explicitly simulated. The multimodal network comprises a road network (generated from Open Street Map) and a transit network (generated from the General Transit Feed Specification, GTFS), including approximately 354,000 links. Considering the scale of LA County (more than 10 million populations in 2016), 10% of the population is simulated in MATSim, and the roadway capacity is calibrated accordingly. The heavy-duty truck trips are also simulated in the road network with passenger cars. A heavy-duty truck is converted to passenger car equivalents (PCE) to account for the effects of trucks on link capacity in the mixed traffic flow. In the simulation, a truck is regarded as a 3.5 PCE.

The validation results of the simulation model are present in Figure A6. Freeways with top 10 daily volumes in LA County are selected as reference, and historical traffic count data are obtained from the Performance Measurement System (PeMS) as the validation data set.

4.3 Emission Inventory Development

4.3.1 Scenario Development

The county-level and source-specific emission data except the mobile sources are collected from California Emissions Projection Analysis Model (CEPAM2019 v1.03)[34] with a base year of 2017. For mobile source (both on-road and off-road sectors), we used EMFAC2021 v1.0.2[33], which is an updated version as compared to the EMFAC2017 embedded in CEPAM2019. For the Base, Disparity, and Equity scenarios, we adjusted the emission for upstream and downstream energy use and production changes due to increased ZEVs population. For Equity_MSS scenario, we further adjusted the medium- and heavy-duty vehicle ZEVs penetration rate and off-road emission rates using EMFAC META model[33], which is created based on CARB 2020 MSS[1] document. We used CARB default settings for the META model.

4.3.2 Emission Inventory Development for On-road Sector

Based on the ZEVs ownership percentage in a specific census tract in 2035, we assume that the same percentage of trips originating from the census tract will be ZEVs trips. The ZEVs trips are randomly selected from all trips originating from a census tract.

We then aggregate link-level hourly emission rates for $PM_{2.5}$ and NO_X. On-road emission rates for LA County are retrieved from EMFAC2021 v1.0.2[33], an official emission inventory database developed by the CARB. Vehicle category-specific emission rates from EMFAC are matched with vehicle types in the MATSim model by vehicle weight class (Table A2). Unlike EMFAC, which uses a more detailed vehicle category classification, the MATSim model only classifies vehicles into four vehicle weight-based categories. Thus, we calculate MATSim-weighted emission rates from EMFAC using the equation below:

$$ER_MATSIM_j^i = \sum ER_EMFAC_k^i \times VP^k \quad \text{(Eq 4.3 -1)}$$

where $ER_MATSIM_j^i$ stands for the emission rate of pollutant i for MATSim weight class j, $ER_EMFAC_k^i$ stands for the emission rate of pollutant i for EMFAC vehicle category k that falls into MATSim weight class j, and VP^k stands for the vehicle population proportion of EMFAC vehicle category k with regard to the total vehicle population that falls into MATSim weight class j.

Emission rates are then matched with link-level hourly vehicle volumes and vehicle activities (starting or stopping a vehicle) to calculate emissions from different emission processes, including running exhaust emissions, start exhaust tailpipe emissions, and brake and tire wear emissions. The emissions from all processes are then aggregated together to reflect the total emissions of a specific link. We then convert the link-level data into grid cells that represent the spatial emission inventory pattern, which is subsequently incorporated into the chemical transport model for ambient air quality simulation.

4.3.3 Emission Inventory Development for Upstream and Downstream Production

As the future ZEVs population will increase the demand for electricity from the electricity generating sector while simultaneously reducing reliance on oil and gas production, it is essential to adjust the emissions from these two sectors accordingly. Therefore, we modify the emissions projections for both the electricity generating units and oil and gas production sectors based on the anticipated ZEVs population in 2035, ensuring a more accurate reflection of their environmental impact. We modified the stationary emissions from petroleum and gas industry for all 2035 scenarios. The overall Petroleum industry scaling down factor is calculated using the following equation:

$$Scaling\ Down\ Factor = \frac{\text{REAL Scenario EMFAC 2035 PC}}{\text{BAU Scenario EMFAC 2035 PC}} \times Onroad\ \% \qquad \text{(Eq 4.3 -2)}$$

where the PC stands for Petroleum Consumption (includes the gasoline, diesel, and gas energy consumption) from on-road vehicles in EMFAC 2035 database under different scenarios, Onroad% stands for the on-road transportation sector consumption percentage. Based on a report from the U.S. Energy Information Administration[35] in year 2019, 68% petroleum is used in the on-road transportation sector. The final scaling down factor for the petroleum and gas industry is

0.80 for Disparity and Equity scenarios and 0.78 for Equity_MSS scenario, assuming the emission factors and the on-road petroleum consumption percentage stay the same in 2035.

Similarly, we also modify the emissions from the electric generating units. We first obtain the 2017 California electricity net generation data from the Energy Information Administration[36].We then apply activity growth factor from CEPAM to project the electricity net generation data in 2035. The overall scaling up factor for electric generating units was calculated using the following equation:

$$Scaling\ Up\ Factor = \frac{E_{onroad} + E_{net}}{E_{net}} \qquad \text{(Eq 4.3 -3)}$$

Where the E_{onroad} stands for the electricity needed from the on-road transportation sector and E_{Net} stands for the projected net electricity generation in year 2035. The final scaling up factor is 1.20 for Disparity and Equity Scenarios, and 1.21 for Equity_MSS scenario. While our scaling-up calculation method for estimating emissions from electric generating units serves as a useful proxy, it is important to note that it remains a rough approximation due to the complexity involved in modeling the entire energy system. Given our study focuses on equity strategies, we have prioritized other aspects of the analysis, and we do not anticipate that uncertainties in energy system estimation will affect our main conclusions on equity analysis.

We utilized emission factors for power plants in LA City from the previous LA100 study[37], specifically adopting those from the Early & No Biofuels Scenario. In this scenario, emissions stem solely from NOx and NH_3, as power plants have transitioned to using hydrogen as their fuel source, significantly altering their emission profiles.

4.4 Air Quality Modeling

We use WRF-Chem version 3.9.1, a fully coupled meteorology-chemistry model that considers highly nonlinear and complex meteorological and atmospheric chemistry processes. The simulations are conducted for January, April, July, and October, representing winter, spring, summer, and fall, respectively. We apply the model to three nested domains (Figure 10): Domain 1 covers the western United States and its surrounding areas at a 12 × 12 km^2 horizontal resolution; Domain 2 covers Southern California with a 4 × 4 km^2 resolution; and Domain 3 covers LA County with a high resolution of 1.33 × 1.33 km^2.

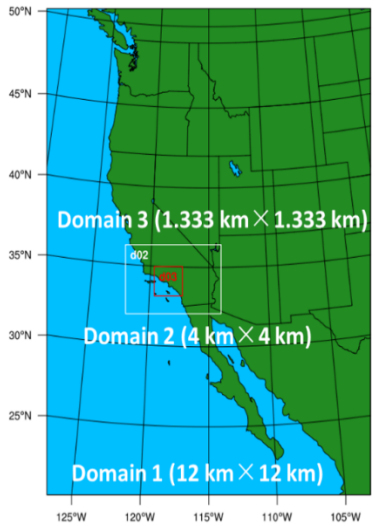

Figure 10. Illustration of triple nested modeling domains used in this study

The vertical resolution of the WRF-Chem includes 24 layers from the surface to 100 hPa, with denser layers at lower altitudes to resolve the planetary boundary layer. We employ an extended Carbon Bond 2005 with chlorine chemistry coupled with the Modal for Aerosol Dynamics in Europe/Volatility Basis Set (MADE/VBS). MADE/VBS uses a modal aerosol size representation and an advanced secondary organic aerosol module based on the VBS approach. The aqueous-phase chemistry is based on the AQChem module used in the Community Multiscale Air Quality model[38]. The National Centers for Environmental Prediction Final Analysis (NCEP-FNL) reanalysis data in year of 2017 was used to force the meteorology initial and boundary conditions for all simulations, which is able to isolate changes in air pollution resulting from future emissions changes, without additional confounding factors such as changing meteorology or climate.

As described above, we obtain the county-level, source-specific anthropogenic emissions from the CARB CEPAM estimations and then convert the county-level emissions into 1.33 × 1.33 km^2 gridded data based on high-resolution spatial distribution information provided by the California Nexus project[39].The on-road transportation emission maps are based on the ZEVs ownership and the MATSim simulated trips in each year, as mentioned above. We then distribute the CEPAM on-road emission estimation in each county in the corresponding years to the grid level following the new emission map. The biogenic emissions are calculated online using the Model of Emissions of Gases and Aerosols from Nature[40]. Dust emissions are calculated online, based on the Goddard Chemical Aerosol Radiation Transport dust emission scheme[41]. Sea-salt emission calculation follows parameterization in a previous study[42].

We compared the simulated and observed monthly average $PM_{2.5}$ concentrations and monthly average of daily MDA8 O_3 concentrations at each individual monitoring site over Southern California (shown in Figure A1). The observed O_3 concentrations were obtained from the U.S. EPA AQS, and the data were converted to MDA8 O_3 concentrations. Daily averaged $PM_{2.5}$ concentrations for the innermost domain were also gathered from AQS. We evaluated the model performance against these observations using various statistical measures, including normalized mean bias (NMB), normalized mean error (NME), mean fractional bias (MFB), and mean

fractional error (MFE), which are listed in Table A3. The evaluation benchmarks suggested by the EPA and previous studies are also summarized in Table A3.

The model generally reproduces the magnitude and spatial distribution of $PM_{2.5}$ concentrations, with an overall slight overestimation of 2% in January and underestimation in the other three seasons of 5%, 25%, and 9% in April, July, and October, respectively. The performance statistics for $PM_{2.5}$ meet the model performance goal (MFB within ±30% and MFE ≤ 50%) in all months, indicating an overall good model-measurement agreement. For O_3, the model is able to capture the spatial variability but slightly overestimates the MDA8 O_3 concentrations in January by 4% on average and underestimates it in the other three seasons by 9%, 15%, and 10% in April, July, and October, respectively. The overall performance statistics for O_3 concentration meet the model performance criteria (i.e., NMB within ±15% and NME < 25%), indicating a generally good agreement between the model and measurements.

4.5 Public Health Benefits Assessment

The Environmental Benefits Mapping and Analysis Program - Community Edition (BenMAP-CE) is a versatile and widely-used tool developed by the U.S. EPA[43]. BenMAP-CE is designed to estimate the health benefits and potential economic value associated with improvements in air quality, particularly those resulting from policy interventions or changes in emission sources. The program uses spatially-resolved air quality data, along with concentration-response functions and population data, to assess the health impacts of changes in air pollution levels. By quantifying the number of avoided premature deaths, respiratory illnesses, hospitalizations, and other health outcomes, BenMAP-CE enables policymakers and researchers to better understand the implications of various air quality improvement strategies.

We used BenMAP-CE v1.5, the latest version published in March 2023 for our analysis. Drawing upon the changes in ambient concentrations of air pollutants simulated by the WRF-Chem model for the scenarios, we estimate the health impacts associated with $PM_{2.5}$ and O_3, focusing on changes in mortality and morbidity. This analysis provides a clearer understanding of the potential consequences of different ZEVs adoption scenarios on public health. The following equations are used to calculate the health impact,

$$HR = e^{\beta \Delta Y} \qquad \text{(Eq 4.5 -1)}$$

$$AF = \frac{HR-1}{HR} = 1 - e^{-\beta \Delta X} \qquad \text{(Eq 4.5 -2)}$$

$$\Delta Impact = y_0\left(1 - e^{\beta \Delta X}\right) Pop. \qquad \text{(Eq 4.5 -3)}$$

where ΔX is the pollution-specific concentration change based on scenarios, β is the exposure-response factor, HR is the hazard ratio found in relevant epidemiologic study which uses ΔY, a 10 ppb and 10 μg/m^3 value that links the change in cause-specific mortality rates to incremental O_3 and $PM_{2.5}$ exposure, respectively, AF stands for the attributable fraction of the disease specific mortality attributable to a certain air pollutant, $\Delta Impact$ is the estimated changes in health impacts incidences, y_0 is the baseline incidences, and Pop. is the population studied.

We used the BenMAP-CE v1.5 default baseline incidences rates (y_0) for our analysis. For mortality, BenMAP-CE projected baseline incidences rate to 2035 for each racial and ethnic group. For morbidity, the available data are limited to 2014 for each racial and ethnic group, as BenMAP-CE v1.5 does not include projections for 2035. Consequently, our morbidity analysis is based on the 2014 data. For population (Pop.), we utilized the 2035 projected population data available within BenMAP-CE.

In order to select appropriate epidemiological studies for our analysis, we ensured that the selected studies are up-to-date with the most recent EPA guidelines on health impact assessment and comply with the EPA Standard Health Functions, which were updated in 2021. This ensures that our analysis adheres to the latest recommendations and best practices in the field.
Table 5 lists the exposure-response factors we used in this study.

Table 5. Exposure-response Factors Used

Pollutant	Category	Health Endpoint	Author	Metric	Beta type	Age Range
$PM_{2.5}$	Long-term mortality	All-cause mortality	Pope et al. (2019)[44]	D24HourMean	Uniform and racial/ethnic specific	18-99
	Morbidity	ER visit - Respiratory	Krall et al. (2016)[45]	D24HourMean	Uniform only	0-99
O_3	Long-term mortality	All-cause mortality	Turner et al. (2016)[46]	D8HourMax	Uniform only	30-99
	Morbidity	ER visit - Respiratory	Barry et al. (2018)[47]	D8HourMax	Uniform only	0-99

4.6 Monetization of Public Health Benefits

To determine the worth of the health benefits, we employ a methodology that involves assigning monetary values to the estimated health outcomes derived from our previous steps. To achieve this, we use BenMAP-CE v1.5 which allows us to quantify the financial value of these health outcomes. First, we identify appropriate valuation functions from 2021 EPA Standard Health Functions database[43], which are derived from relevant economic studies or guidelines. These valuation functions typically express the economic value of health outcomes in terms of dollars per unit (e.g., dollars per avoided premature death, hospitalization, or respiratory illness). Valuation functions used are listed in Table 6.

Table 6. Valuation Functions Selected from BenMAP-CE v1.5

Endpoint	Reference	Value (2015$)
Mortality	VSL based on 26 studies, no discount rate applied	$8,700,000
ER visit - Respiratory	Healthcare Cost and Utilization Project	$875

We then apply the selected valuation functions to the estimated health outcome changes for each scenario. This involves multiplying the change in health outcomes (e.g., avoided premature deaths, hospitalizations) by the corresponding monetary values per unit, as provided by the valuation functions. Finally, we calculate the total monetized health benefits by summing the

monetized health benefits across all health endpoints for each scenario comparison. This provides a comprehensive understanding of the economic impact associated with the changes in air quality due to different ZEVs adoption scenarios.

5 References

1. California Air Resources Board. 2020 Mobile Source Strategy. https://ww2.arb.ca.gov/resources/documents/2020-mobile-source-strategy (2021).

2. California Air Resources Board. 2016 Mobile Source Strategy. https://ww2.arb.ca.gov/resources/documents/2016-mobile-source-strategy (2016).

3. Beelen, R. *et al.* Natural-cause mortality and long-term exposure to particle components: An analysis of 19 European cohorts within the multi-center ESCAPE project. *Environ. Health Perspect.* **123**, 525–533 (2015).

4. Khreis, H. *et al.* Exposure to traffic-related air pollution and risk of development of childhood asthma: A systematic review and meta-analysis. *Environ. Int.* **100**, 1–31 (2017).

5. Boogaard, H. *et al.* Long-term exposure to traffic-related air pollution and selected health outcomes: A systematic review and meta-analysis. *Environ. Int.* **164**, (2022).

6. Raju, A. S. K., Wallerstein, B. R. & Johnson, K. C. Achieving NOx and Greenhouse gas emissions goals in California's Heavy-Duty transportation sector. *Transp. Res. Part D-Transport Environ.* **97**, (2021).

7. Forrest, K., Lane, B., Tarroja, B., Mac Kinnon, M. & Samuelsen, S. Emissions and air quality implications of enabling on-road vehicles as flexible load through widescale zero emission vehicle deployment in California. *Transp. Res. Rec.* (2022) doi:10.1177/03611981221121259.

8. Garcia, E., Johnston, J., McConnell, R., Palinkas, L. & Eckel, S. P. California's early transition to electric vehicles: Observed health and air quality co-benefits. *Sci Total Env.* **867**, 161761 (2023).

9. Pan, S. *et al.* Impacts of the large-scale use of passenger electric vehicles on public health in 30 US. metropolitan areas. *Renew. Sustain. Energy Rev.* **173**, (2023).

10. Lieven, T. Policy measures to promote electric mobility - A global perspective. *Transp. Res. Part a-Policy Pract.* **82**, 78–93 (2015).

11. Axsen, J., Hardman, S. & Jenn, A. What do we know about zero-emission vehicle mandates? *Environ. Sci. Technol.* **56**, 7553–7563 (2022).

12. Department for Transport U.K. Transitioning to zero emission cars and vans: 2035 delivery plan. *Gov.UK* 57 https://www.gov.uk/government/publications/transitioning-to-

zero-emission-cars-and-vans-2035-delivery-plan (2021).

13. Ou, S. Q. *et al.* The dual-credit policy: Quantifying the policy impact on plug-in electric vehicle sales and industry profits in China. *Energy Policy* **121**, 597–610 (2018).

14. Greene, D. L., Park, S. & Liu, C. Z. Public policy and the transition to electric drive vehicles in the U.S.: The role of the zero emission vehicles mandates. *Energy Strateg. Rev.* **5**, 66–77 (2014).

15. Office of Governor Gavin Newsom. Executive Order N-79-20. *Executive Department, State of California* (2020).

16. McConnell, V. & Leard, B. Pushing New Technology into the Market: California's zero emissions vehicle mandate. *Rev. Environ. Econ. Policy* **15**, 169–179 (2021).

17. Lane, B., Shaffer, B. & Samuelsen, S. A comparison of alternative vehicle fueling infrastructure scenarios. *Appl. Energy* **259**, (2020).

18. Davis, A. W. & Tal, G. Investigating the sensitivity of electric vehicle out-of-home charging demand to changes in light-duty vehicle fleet makeup and usage: A case study for California 2030. *Transp. Res. Rec.* **2675**, 1384–1395 (2021).

19. Ledna, C., Muratori, M., Brooker, A., Wood, E. & Greene, D. How to support EV adoption: Tradeoffs between charging infrastructure investments and vehicle subsidies in California. *Energy Policy* **165**, (2022).

20. Kawamura, K. & Kaplan, I. R. Motor Exhaust emissions as a primary source for dicarboxylic-acids in Los-Angeles ambient air. *Environ. Sci. Technol.* **21**, 105–110 (1987).

21. Zhu, Y. F., Fung, D. C., Kennedy, N., Hinds, W. C. & Eiguren-Fernandez, A. Measurements of ultrafine particles and other vehicular pollutants inside a mobile exposure system on Los Angeles freeways. *J. Air Waste Manage. Assoc.* **58**, 424–434 (2008).

22. Sowlat, M. H., Hasheminassab, S. & Sioutas, C. Source apportionment of ambient particle number concentrations in central Los Angeles using positive matrix factorization (PMF). *Atmos. Chem. Phys.* **16**, 4849–4866 (2016).

23. Evans, M. C., Bazargan, M., Cobb, S. & Assari, S. Pain intensity among community-dwelling African American older adults in an economically disadvantaged area of Los Angeles: Social, behavioral, and health determinants. *Int. J. Environ. Res. Public Health* **16**, (2019).

24. Wilhelm, M. & Ritz, B. Residential proximity to traffic and adverse birth outcomes in Los Angeles County, California, 1994-1996. *Environ. Health Perspect.* **111**, 207–216 (2003).

25. Westerdahl, D., Fruin, S., Sax, T., Fine, P. M. & Sioutas, C. Mobile platform

measurements of ultrafine particles and associated pollutant concentrations on freeways and residential streets in Los Angeles. *Atmos. Environ.* **39**, 3597–3610 (2005).

26. Fruin, S., Westerdahl, D., Sax, T., Sioutas, C. & Fine, P. M. Measurements and predictors of on-road ultrafine particle concentrations and associated pollutants in Los Angeles. *Atmos. Environ.* **42**, 207–219 (2008).

27. Winter, P. L., Padgett, P. E., Milburn, L. A. S. & Li, W. M. Neighborhood parks and recreationists' exposure to ozone: A comparison of disadvantaged and affluent communities in Los Angeles, California (vol 63, pg 379, 2019). *Environ. Manage.* **63**, 836 (2019).

28. Boeing, G., Lu, Y. G. & Pilgram, C. Local inequities in the relative production of and exposure to vehicular air pollution in Los Angeles. *Urban Stud.* (2023) doi:10.1177/00420980221145403.

29. Liang, X. *et al.* Air quality and health benefits from fleet electrification in China. *Nat. Sustain.* **2**, 962–971 (2019).

30. Peters, D. R., Schnell, J. L., Kinney, P. L., Naik, V. & Horton, D. E. Public health and climate benefits and trade-offs of US vehicle electrification. *Geohealth* **4**, (2020).

31. Skipper, T. N., Lawal, A. S., Hu, Y. T. & Russell, A. G. Air quality impacts of electric vehicle adoption in California. *Atmos. Environ.* **294**, (2023).

32. California Office of Environmental Health Hazard Assessment. SB 535 Disadvantaged Communities. *OEHHA* https://oehha.ca.gov/calenviroscreen/sb535 (2022).

33. California Air Resources Board. EMission FACtor (EMFAC) 2021. https://arb.ca.gov/emfac/ (2021).

34. California Air Resources Board. CEPAM2019v1.03 - Standard Emission Tool. https://ww2.arb.ca.gov/applications/cepam2019v103-standard-emission-tool (2021).

35. U.S. EIA. California - State Energy Profile Overview - U.S. Energy Information Administration (EIA). https://www.eia.gov/state/?sid=CA (2021).

36. U.S. EIA. State Electricity Profiles - 2017. (2019).

37. Heath, G., Ban-Weiss, G., Li, Y., Zhang, J. & Ravi, V. LA 100 Study Chapter 9. (2021).

38. Wang, K., Zhang, Y., Yahya, K., Wu, S. Y. & Grell, G. Implementation and initial application of new chemistry-aerosol options in WRF/Chem for simulating secondary organic aerosols and aerosol indirect effects for regional air quality. *Atmos. Environ.* **115**, 716–732 (2015).

39. US Department of Commerce, N. E. S. R. L. C. S. L. NOAA ESRL CSD Projects: CalNex 2010.

40. Guenther, A. *et al.* Estimates of global terrestrial isoprene emissions using MEGAN (Model of Emissions of Gases and Aerosols from Nature). *Atmos. Chem. Phys.* **6**, 3181–3210 (2006).

41. Ginoux, P. *et al.* Sources and distributions of dust aerosols simulated with the GOCART model. *J. Geophys. Res. Atmos.* **106**, 20255–20273 (2001).

42. Gong, S. L. A parameterization of sea-salt aerosol source function for sub- and super-micron particles. *Global Biogeochem. Cycles* **17**, 1097 (2003).

43. US EPA. Environmental Benefits Mapping and Analysis Program - Community Edition (BenMAP-CE). *US Environmental Protection Agency* Last updated on May 18 https://www.epa.gov/benmap (2023).

44. Pope, C. A. *et al.* Mortality risk and fine particulate air pollution in a large, representative cohort of U.S. adults. *Environ. Health Perspect.* **127**, (2019).

45. Krall, J. R. *et al.* Associations between source-specific fine particulate matter and emergency department visits for respiratory disease in four U.S. cities. *Environ. Health Perspect.* **125**, 97–103 (2017).

46. Turner, M. C. *et al.* Long-term ozone exposure and mortality in a large prospective study. *Am. J. Respir. Crit. Care Med.* **193**, 1134–1142 (2016).

47. Barry, V. *et al.* Characterization of the concentration-response curve for ambient ozone and acute respiratory morbidity in 5 U.S. cities. *J. Expo. Sci. Environ. Epidemiol.* **29**, 267 (2019).

6 Appendix

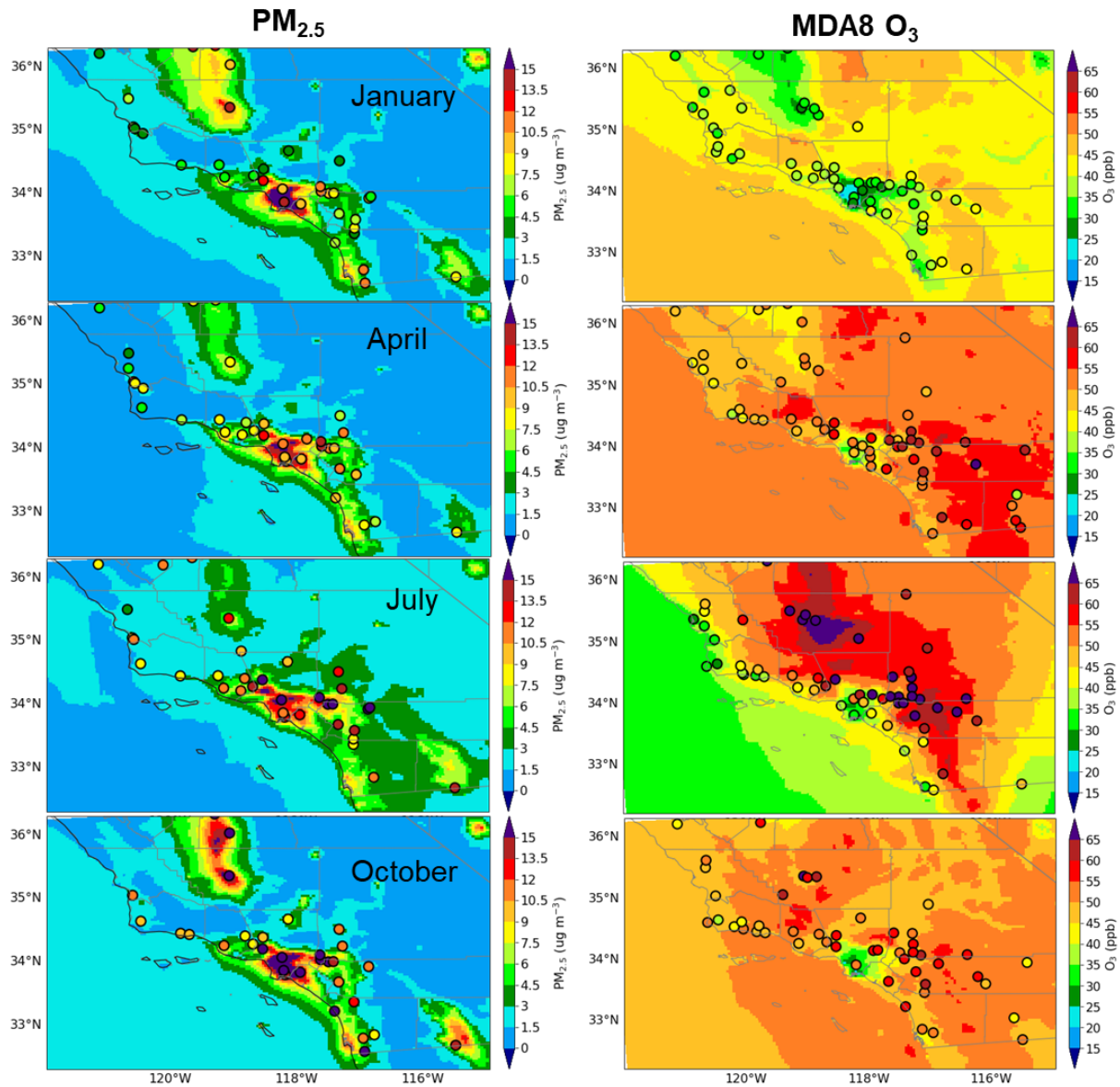

Figure A1. Observed (dots) and simulated (contours) monthly mean $PM_{2.5}$ concentrations (left), and monthly mean daily maximum 8-h O_3 concentrations (MDA8 O_3, right) over south California in January, April, July, and October 2017

The observations are from US EPA Air Quality System (AQS).

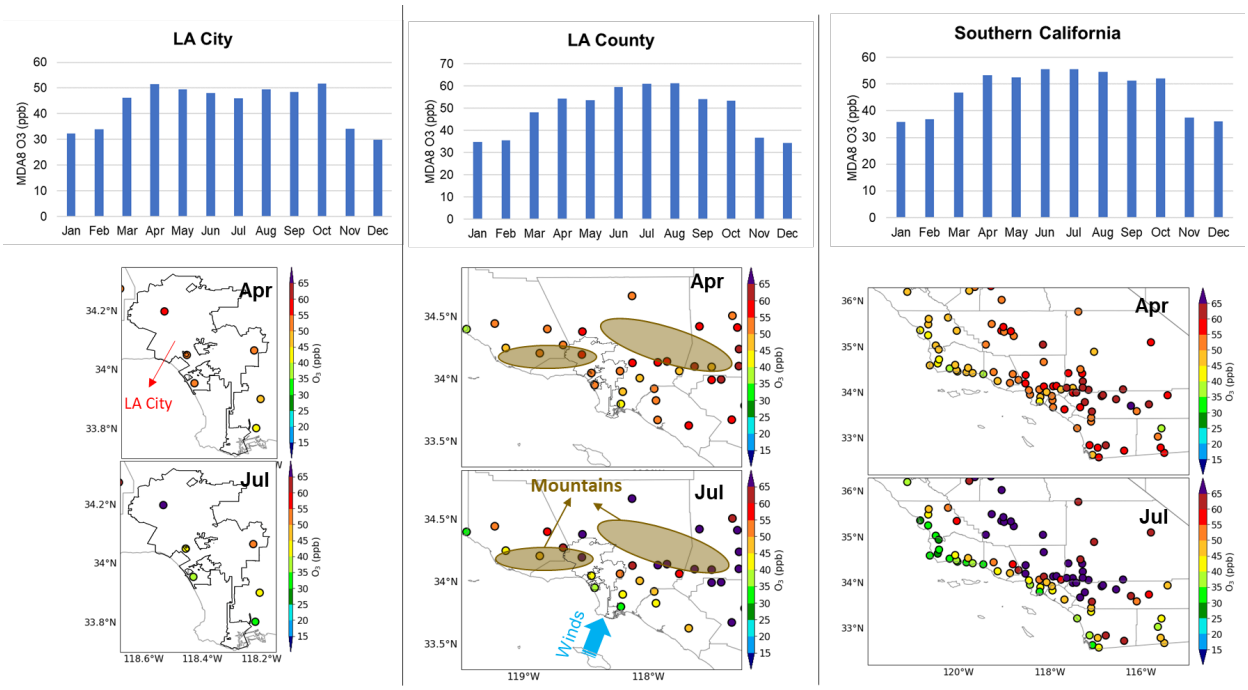

Figure A2. First row shows the seasonal variations of MDA8 O_3 concentrations over LA City, LA County, and Southern California based on EPA AQS observations (https://www.epa.gov/aqs). Second row shows the corresponding spatial distribution of AQS observed O_3 concentrations in April and July.

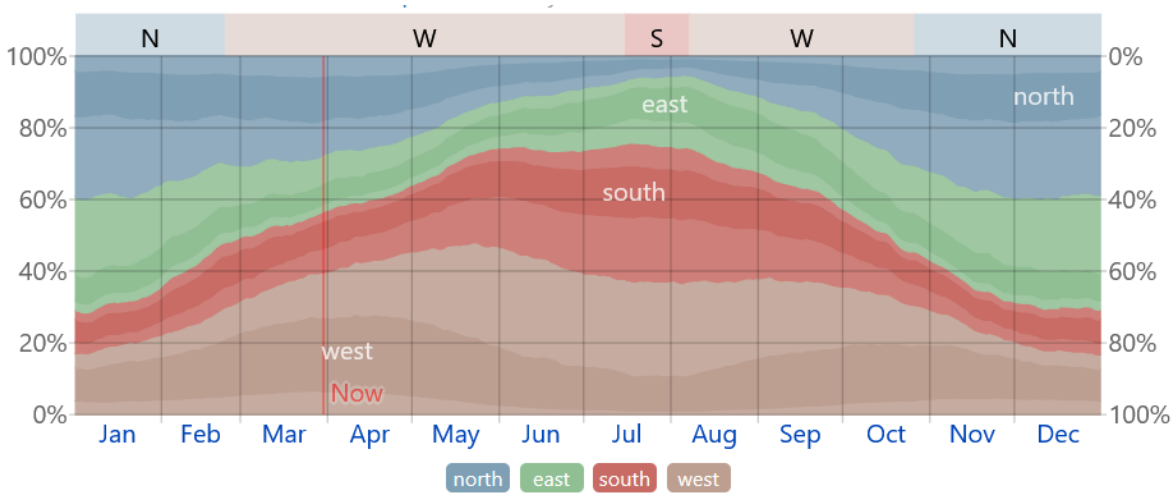

Figure A3. Wind direction climatology in Los Angeles (adapted from https://weatherspark.com/y/1705/Average-Weather-in-Los-Angeles-California-United-States-Year-Round#Figures-WindDirection)

Note that westerly and southerly are prevailing in summer months.

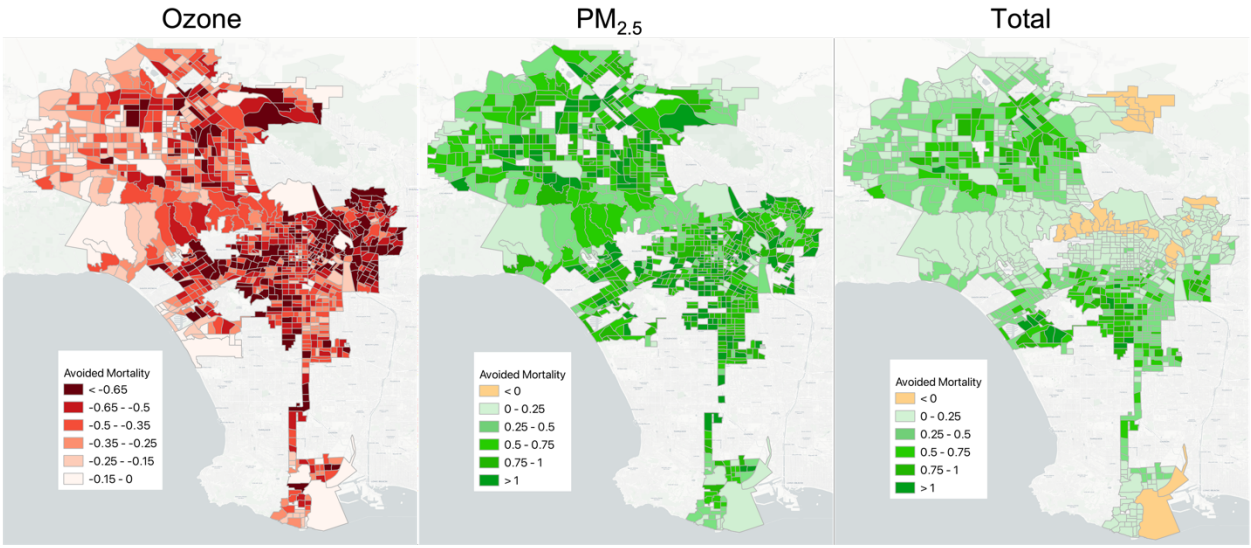

Figure A4. Avoided mortality between Equity_MSS and Base scenarios

From left to right: Ozone-related, $PM_{2.5}$-related, and total avoided mortality. Ozone-related avoided mortality values are negative, indicating disbenefits due to increased ozone concentrations.

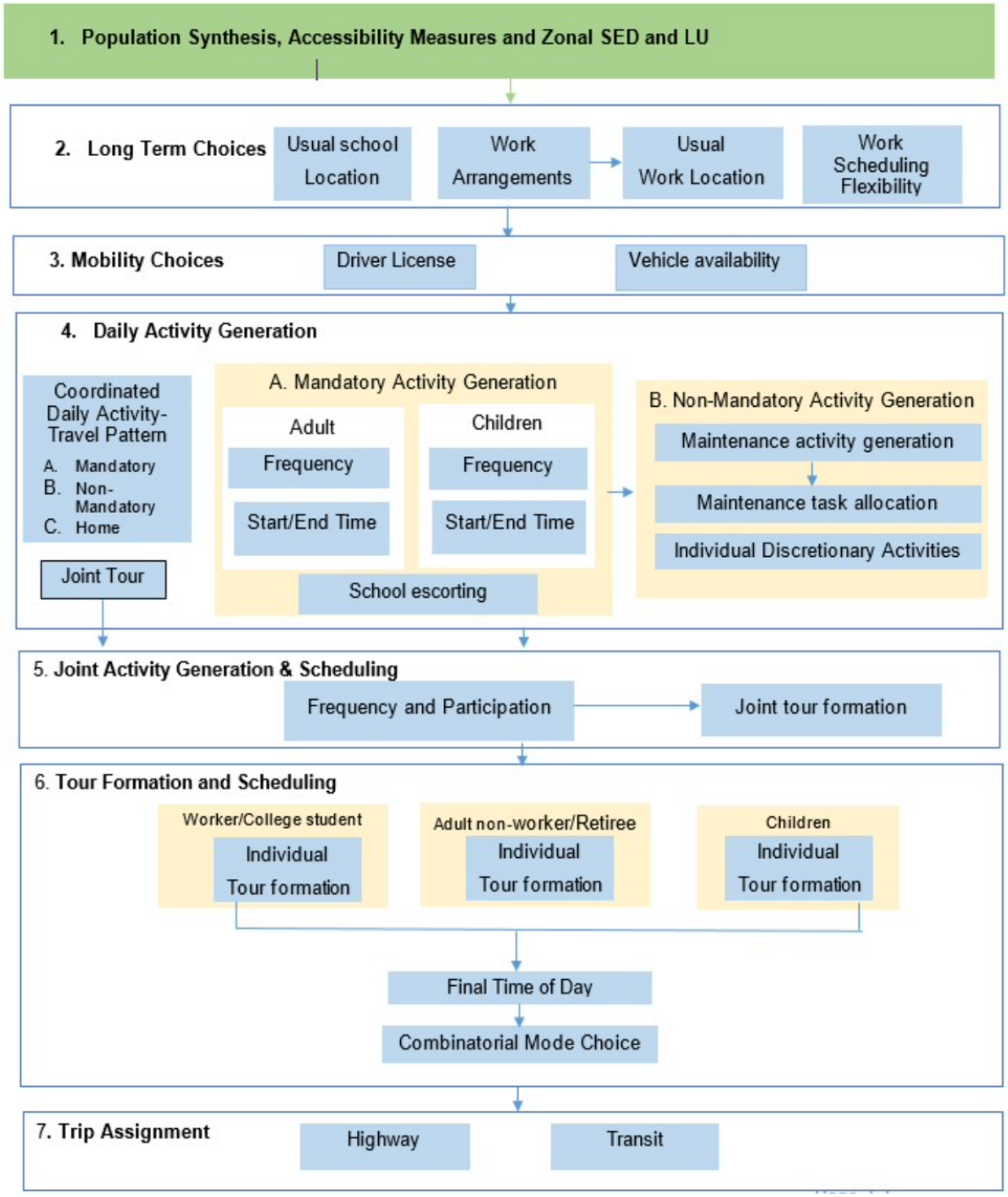

Figure A5. System design of the SCAG ABM (SCAG, 2020)

SED=Socio-economic and demographic, LU=Land use

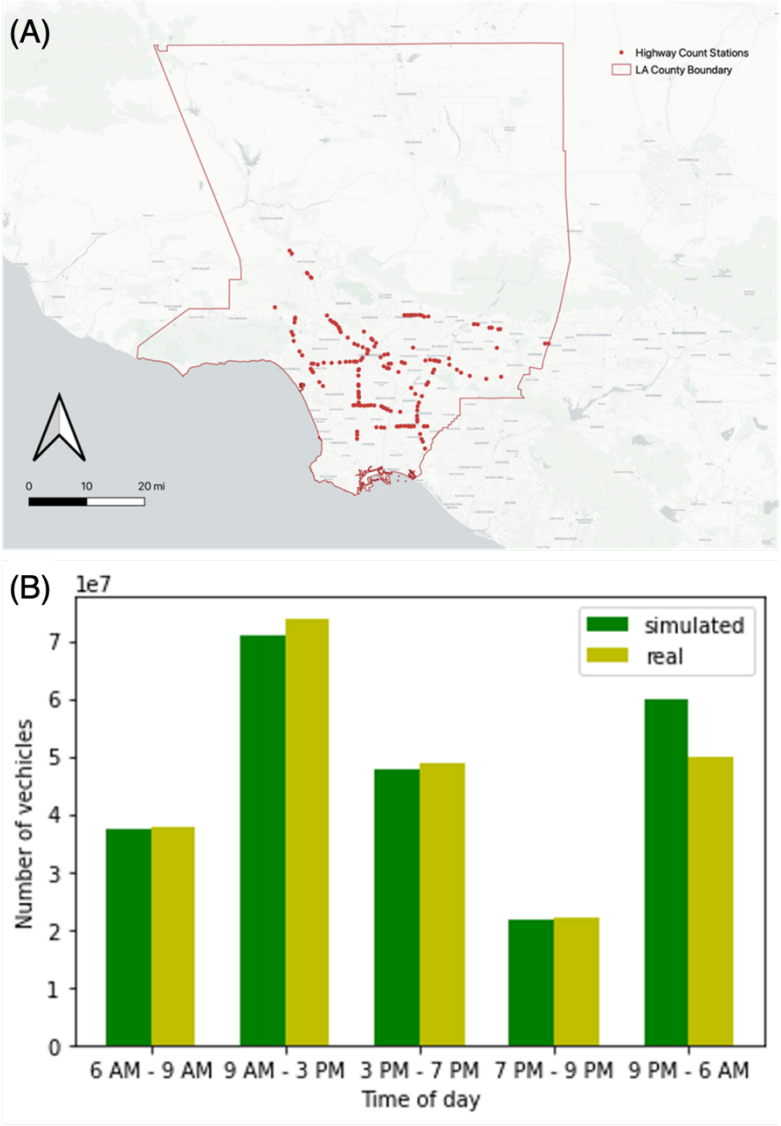

Figure A6. (A) Traffic count locations selected across Los Angeles County; (B) Comparison of simulated and real traffic volumes in Los Angeles County

Table A1. Technical Specifications of Scenarios Analyzed in This Study

	LA 100 Early & No Biofuels - High	LA 100 ES UCLA[1]		
Time	2035	2035 ZEV Disparity	2035 ZEV Equity	2035 ZEV Equity (more MD-HD) (MSS)
Energy Profile	100% clean[2] energy	100% clean[2] energy	100% clean[2] energy	100% clean[2] energy
	On-road Transportation Electrification Profile			
Light-duty	50%	50%	50%	50%
Medium-duty	0%	15.6%[3]	15.6%[3]	22%
Heavy-duty	0%	19.6%[3]	19.6%[3]	39%
School and urban buses	100%	EMFAC	EMFAC	100%
	On-road Transportation Emission Spatial Distribution			
Passenger Vehicle Medium-duty Heavy-duty School and urban buses	Equally distributed	Emission reduction map based on (1) ZEV ownership and (2) the MATSim simulated trips	Equally distributed	Equally distributed
	ZEV Fleet Profile (LDV / MDV / HDV)[4]			
PHEV	50%	25% / 0% / 0%		
BEV	50%	67% / 100% / 100%		
FCEV	0%	8% / 100% / 100%		
	Off-road Transportation[5]			
Heavy-duty in ports	100%	No data in EMFAC	No data in EMFAC	No data in EMFAC
Ocean-going Vessels	90%	EMFAC 2035 Original	EMFAC 2035 Original	EMFAC META Off-road (https://arb.ca.gov/emfac/meta/off-road, check "?" for detailed supporting regulations) MSS
Cargo Handling Equipment	100%			
Commercial Harbor Craft	N/A			
Construction, Mining, Industrial	N/A			
Forklift	N/A			
Airport GSE	N/A			
Locomotive	N/A			
Recreational Marine Vessel	N/A			
Small Off-road Engine	N/A			
Transport Refrigerator Unit	N/A			
	Buildings Electrification			
Commercial	Scaling factor ~3-5%	N/A	N/A	N/A
Residential	Scaling factor ~12-15%	N/A	N/A	N/A
	Oil & Gas Industry			
Demand Reduction	N/A	Scale down based on ZEV population		

1. Electrification %s for LA 100 ES (if not specified) are in line with CARB most recent MSS (2020), and a recent CEC report (2021, https://efiling.energy.ca.gov/getdocument.aspx?tn=238853)
2. "clean energy" defined as no natural gas generation or biofuels. Natural gas electricity generation are replaced with gas electricity generation with wind, solar and battery storage. LA city has approved LA100 Early & No Biofuels (https://www.utilitydive.com/news/la-approves-100-clean-energy-by-2035-target-a-decade-ahead-of-prior-goal/605980/)
3. Based on EMFAC V2021.
4. For MDV and HDV, we assume 100% BEV and FCEV. During emission calculation, BEV and FCEV will both generate zero tailpipe emissions.
5. Will be equally distributed into "Area" source in WRF-Chem, "Aircraft" has specific spatial emission inventory

Table A2. Correspondence Between MATSim and EMFAC Vehicle Categories

MATSim Vehicle Type	Passenger Vehicles	Light-heavy Truck	Medium-heavy Truck	Heavy-heavy Truck
Corresponding Weight Class	< 8,500 lbs GVW	8,500 to 14,000 lbs. GVW	14,001 to 33,000 lbs. GVW	>33,000 lbs. GVW
EMFAC Vehicle Category	"LDA", "LDT1", "LDT2", "MDV"	"LHD1", "LHD2"	"T6 CAIRP Class 4", "T6 CAIRP Class 5", "T6 CAIRP Class 6", "T6 CAIRP Class 7", "T6 Instate Delivery Class 4", "T6 Instate Delivery Class 5", "T6 Instate Delivery Class 6", "T6 Instate Delivery Class 7", "T6 Instate Other Class 4", "T6 Instate Other Class 5", "T6 Instate Other Class 6", "T6 Instate Other Class 7", "T6 Instate Tractor Class 6", "T6 Instate Tractor Class 7", "T6 OOS Class 4", "T6 OOS Class 5", "T6 OOS Class 6", "T6 OOS Class 7", "T6 Public Class 4", "T6 Public Class 5", "T6 Public Class 6", "T6 Public Class 7", "T6 Utility Class 5", "T6 Utility Class 6", "T6 Utility Class 7", "T6TS"	"T7 CAIRP Class 8", "T7 NNOOS Class 8", "T7 NOOS Class 8", "T7 POAK Class 8", "T7 POLA Class 8", "T7 Public Class 8", "T7 Single Concrete/Transit Mix Class 8", "T7 Single Dump Class 8", "T7 Single Other Class 8", "T7 SWCV Class 8", "T7 Tractor Class 8", "T7 Utility Class 8", "T7IS"

Table A3. Statistics of Model Performance for Chemical Predictions

	Month	Site number	Mean Sim[a]	Mean Obs[b]	NMB[c] (%)	NME[d] (%)	MFB[e] (%)	MFE[f] (%)
$PM_{2.5}$ ($\mu g\ m^{-3}$)	Jan	34	8.2	8.1	2	53	4	39
	Apr	36	8.5	9.0	-5	60	-13	41
	Jul	35	8.1	10.8	-25	47	-21	36
	Oct	31	10.8	13.4	-19	47	-23	36
	Recommended performance benchmarks[*]				<±30	<50	<±30	<±50
MDA8 O_3 (ppb)	Jan	53	37	35	4	18	2	13
	Apr	58	48	53	-9	16	-5	11
	Jul	59	48	57	-15	23	-8	16
	Oct	49	47	53	-10	19	-6	13
	Recommended performance benchmarks[**]				<±15	<25	-	-

[a]Mean Sim stands for the spatially and temporally averaged simulated concentrations at those observation sites; [b]Mean Obs is the spatially and temporally averaged observed concentrations across all observation sites;
[c]NMB is normalized mean bias;
[d]NME is normalized mean error;
[e]MFB is mean fractional bias;
[f]MFE is mean fractional error.
[*]Based on Boylan and Russell (2006);
[**]Based on U.S. Environmental Protection Agency (EPA), https://www3.epa.gov/ttn/scram/guidance/guide/O3-PM-RH-Modeling_Guidance-2018.pdf.

Cover photo from iStock 874139156